



- GLAST - Shake Test 99 Calorimeter Random Vibration Test Report

Erik Swensen and Eric Ponslet
November 30, 1999

Abstract

This test report summarizes the results of the GLAST Shake Test 99 Calorimeter random vibration test. A qualification level random vibration test was performed to ensure the survivability of the calorimeter when subjected to the launch environment. Modal information such as frequency response functions and power spectral density functions are provided along with an analysis to identify mode shapes and estimate damping and quality factors. The report also includes a look at the measured strain levels during sine burst testing. This test has been funded by the Naval Research Laboratory, under contract #19958-PXI-003, with Praxis and HYTEC inc.



Revision Log

Revision	Date	Author	Summary of Revisions/Comments
OI	November 30, 1999	E. Swensen, E. Ponslet	Initial release.
A	April 12, 2000	E. Swensen	Updated document number, added Revision log

Table of Contents

1. Scope	5
2. Test Objective	5
3. Test Article	5
4. Test Facility	6
5. Test Configuration	7
5.1 Calorimeter Coordinate System	7
5.2 Calorimeter/Test Fixture Set-up	8
5.3 Test Fixture/Shaker Table Mounting	10
6. Signature Test Levels	11
7. Sine Burst Test Levels	12
7.1 Input Test Level Defined in Test Plan	12
7.2 Input Test Level Used	13
8. GEVS Specified Random Vibration Test Levels	14
8.1 Full Amplitude Random Vibration Test Level Defined in Test Plan	14
8.2 Full Amplitude Random Vibration Test Level Used	16
9. Instrumentation	17
9.1 Accelerometers	17
9.1.1 Types	17
9.1.2 Mounting Locations	17
9.2 Strain Gage Sensors	20
9.2.1 Types	20
9.2.2 Mounting Locations	21
10. Test Plan Summary	22
11. Vibration Test Results	23
11.1 Transverse Axis Test Results	23
11.1.1 Random Vibration Test	23
11.1.2 Sine Burst Test	28
11.2 Thrust Axis Test Results	31
11.2.1 Random Vibration Test	31
11.2.2 Sine Burst Test	35
12. References	38
13. Appendix A: Test Summary – As Performed	39
13.1 Test Summary for the Transverse Axis	39

13.2	Test Summary for the Thrust Axis.....	40
14.	<i>Appendix B: Accelerometer Locations.....</i>	<i>41</i>
14.1	Vibration Testing Parallel to the Transverse Axis.....	41
14.2	Vibration Testing Parallel to the Thrust Axis.....	43
15.	<i>Appendix C: Strain Gage Sensor Locations.....</i>	<i>45</i>
16.	<i>Appendix D: Mode Identification Results for the Full Amplitude Random Vibration Test.....</i>	<i>47</i>
16.1	Transverse Axis Results.....	47
16.2	Thrust Axis Results.....	51
17.	<i>Appendix E: Strain Results from the Full Amplitude Sine Burst Test.....</i>	<i>54</i>
17.1	Transverse Axis Results.....	54
17.2	Thrust Axis Results.....	55

1. Scope

This test report describes the vibration tests performed on the Shake Test 99 Cesium Iodide (CsI) Calorimeter for the Gamma-ray Large Area Space Telescope (GLAST). HYTEC Inc. and Naval Research Laboratory (NRL) personnel conducted these tests at NRL facilities. The tests were held on September 22nd, 1999 thru September 24th, 1999. This document encompasses the results obtained during the random vibration tests and details the analysis performed to understand the calorimeter response when subjected to the harsh launch environment. The following sections include information about the test objectives, instrumentation and set-up, input levels, test plan and results of the test.

2. Test Objective

The objective of the random vibration test is to qualify the CsI Calorimeter design to the expected mission environment. The Shake Test 99 calorimeter was subjected to the random vibration levels specified in the General Environmental Verification Specification (GEVS), statistically representative of the mission environment, and the structural response was measured. The response measurements are going to be used to qualify the design and calibrate the analytical models used in the design process. The vibration test provides knowledge of the quality of workmanship, reliability of the design, survivability to the launch environment, interface compatibility with the grid and tracker, and structural response of the CsI logs relative to the calorimeter support structure. These issues will be discussed in greater detail within the results section of this report.

3. Test Article

The Shake Test 99 Calorimeter was used in the qualification level random vibration testing. The calorimeter closely represents the concept proposed for the flight unit with some important differences, which will be described later.

The concept is described in detail in “Conceptual Mechanical Design of a CsI Calorimeter for GLAST”^[2]. It consists of a uni-directional compression cell, holding the CsI logs in position by compressing the stack in the vertical direction between two compression panels. The stack includes several layers of compliant silicon rubber to help control the amount of compression, accommodate tolerances in CsI log dimensions, absorb thermal expansion of the CsI, and provide high friction on the outer surfaces of the logs.

The stack is held in compression by 4 containment panels, bolted to the top and bottom compression panels. Those panels have large rectangular cutouts for clearance to the PIN diodes that instrument the logs, and a number of posts that serve as supports for the PC boards and mechanical connection with the outer shear panels. The containment/shear panel assemblies, tied together with those posts form structural sandwich structures that contain and protect the PC boards, and serve as a backup lateral restraints for the CsI logs.

The Shake Test 99 calorimeter differs from the flight unit conceptual design. Three modifications have been made for the test unit. First, the printed circuit (PC) boards have been left out of most of the testing. It is suspected that the PC boards may strike either the shear panels or the containment panels during the test due to large amplitude response at the corners of the PC boards. The shock response of the PC boards striking the containment panels or shear panels may saturate the calorimeter data set with misleading response measurements. A final test was planned to replace the PC boards and repeat the transverse random vibration test, once the calorimeter response has been measured. However, time constraints prohibited this test from being performed.

Second, the bottom compression panel has been manufactured as a solid plate, whereas the flight unit design would use an aluminum honeycomb sandwich construction to minimize weight. All of the assembly features on the solid bottom compression panel have been included to ensure that the shear panels and containment panels are properly fastened and the interfaces identically represent those on the designed flight unit. The solid bottom compression panel is not expected to have any influence on the calorimeter response during the qualification testing that will prohibit these tests from achieving their goals.

Finally, the CsI logs have been replaced with aluminum blocks filled with a brass core. The high cost to manufacture the CsI logs prohibits their use during this level of qualification testing. The aluminum replacement logs were sized to match the physical dimensions of the CsI logs and the brass core is used to adjust the weight of the replacement logs so they match the physical weight of the CsI logs during dynamic tests.

The Shake Test 99 calorimeter was mounted within a test fixture. The test fixture was designed to represent the mechanical interface between both the calorimeter grid (bottom) and tracker subsystem (top). The test fixture has been designed to have a sufficiently large stiffness when compared to the calorimeter so that the measured response of the fixture doesn't couple with the response of the calorimeter at lower frequencies. The exact stiffness was measured during testing.

4. Test Facility

The random vibration tests were conducted at NRL's, Design, Test and Processing Branch (NRL Code 8210) in the Spacecraft Vibration Test Facility (SVTF). NRL laboratory engineers and technicians conducted the tests and HYTEC Inc. engineers supervised the test activities. NRL-GLAST personnel were available to assist with the test activities and management.

Two shakers were available at the SVTF for the calorimeter random vibration tests. A horizontal shaker was used for the transverse axis testing and a vertical shaker was used for the thrust axis testing. The data acquisition system used in the vibration laboratory is a Hewlett Packard (HP) VXI crates and an HP workstation. First order post processing was performed at NRL using IDEAS. The Frequency Response Function (FRF) and Time History data was transferred to HYTEC in MATLAB format for a more detailed analysis. The results of this are described herein.

5. Test Configuration

The Shake Test 99 calorimeter was subjected to a random vibration test for two axes, one parallel to the thrust axis (vertical) and the second along the transverse axis (orthogonal to the thrust axis). The second transverse axis was not subjected to the random vibration test due to the symmetry of the calorimeter.

The test configuration was similar for both test axes. This was intended to reduce the set-up time that was required to change the test axis. The two changes made were to remove the calorimeter/fixture from the transverse shaker and mount it on the vertical shaker for the thrust test. The accelerometer measurement axis was changed for several of the uni-axial accelerometers used in the test. The following sections describe the calorimeter test configuration for both the thrust and transverse axes tests.

5.1 Calorimeter Coordinate System

The Shake Test 99 calorimeter was assigned a local coordinate system to orient the calorimeter with the test axes and measured response axes. Several CsI replacement logs have been constructed with a #8-32 female thread to accept accelerometer mounts. Two opposing sides of the calorimeter have 8 logs each with this feature and the two remaining sides have 4 logs each with this feature. The local coordinate system assigned to the calorimeter is oriented such that the two sides with 8 mounting holes define the X-axis. An imaginary line can be drawn normal to and through both surface planes, thus defining the axis. The two sides with 4 mounting holes each define the Y-axis, orthogonal to the X-axis. The Z-axis is the third orthogonal axis defined by the right-hand Cartesian coordinate system (vertical direction). Figure 5-1 illustrates these axes.

Each side of the calorimeter will be assigned a label to distinguish the 6 sides when referenced herein. The coordinate system origin has been assigned to be at the center of the calorimeter. This will allow us to refer to each containment/shear panel by the normal vector that passes through the face plane, and which side of the origin the panel is located. For example, the +X side, as referred to herein, will be the side with 8 mounting holes on the positive side of the origin (the positive side will be indicated on the test fixture). The -X side will be the side with 8 mounting holes on the negative side of the origin. This is true for the Y axis as well. The top compression panel will be the +Z side and the bottom compression panel will be the -Z side. The calorimeter will be subjected to vibrations along the X-axis for the transverse tests and the Z-axis for the thrust tests.

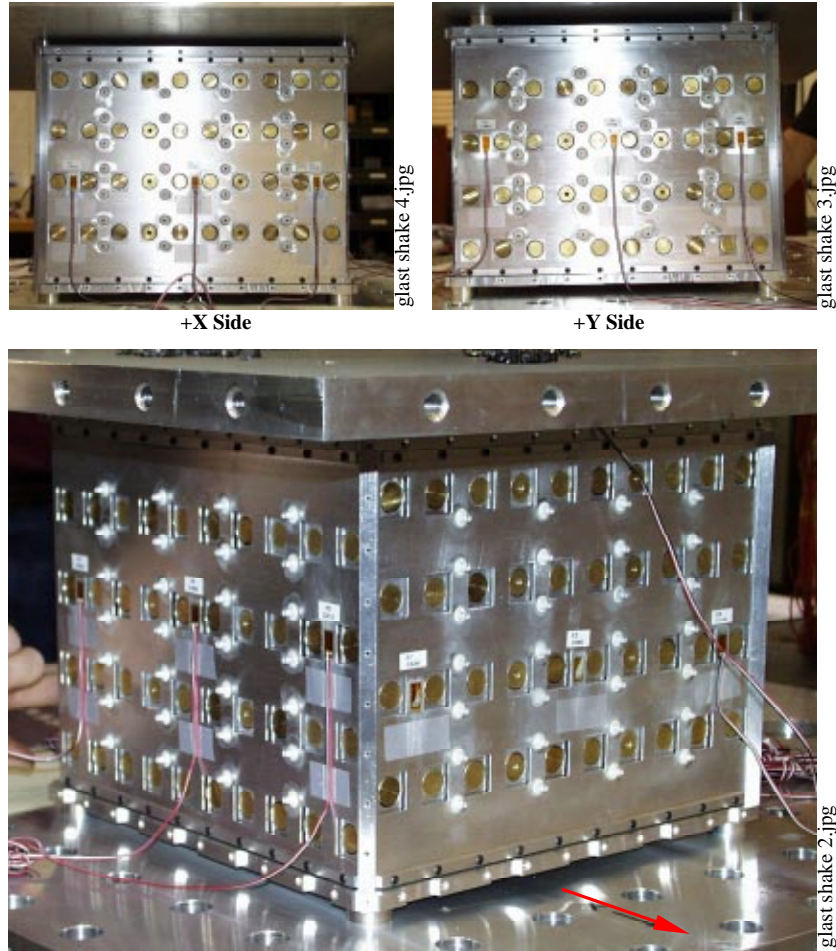


Figure 5-1. The side with eight accelerometer mount locations defines the X axis (Top Left). The side with the 4 accelerometer mount locations defines the Y axis (Top Right). The Cartesian coordinate system is defined using a right-hand coordinate system. The +X axis is illustrated in red and the +Z axis is vertical (Bottom).

5.2 Calorimeter/Test Fixture Set-up

The calorimeter was mounted in a test fixture assembly designed to replicate the mounting configuration of the flight unit. Four mounting surfaces are provided at the top and bottom of the fixture to represent the mounting interface to the grid. The test fixture has been designed with very high stiffness to reduce the response of the calorimeter/test fixture coupled modes.

The calorimeter assembly was mounted in the test fixture at HYTEC Inc. prior to shipping to NRL. The calorimeter was placed on the fixture base plate separated by the four lower spacers. It was secured to the fixture base plate using four ½" x 5/8" long shoulder bolts and torqued to 20 ft-lbs. The threads were coated with medium strength Loctite™ to keep them from coming loose during testing. The medium strength Loctite™ is not a permanent bond and can be separated if required.

The top plate was lowered onto the calorimeter, separated by the four upper spacers. The top plate was aligned with the four mounting locations and secured with

four 5/16" x 5/8" long shoulder bolts and torqued to 64 in-lbs. The threads were also coated with medium strength Loctite™ to keep them from coming loose during testing. Figure 5-2 shows the calorimeter mounted between the test fixture top and bottom plates. The sidewalls have been removed for illustrative purposes.

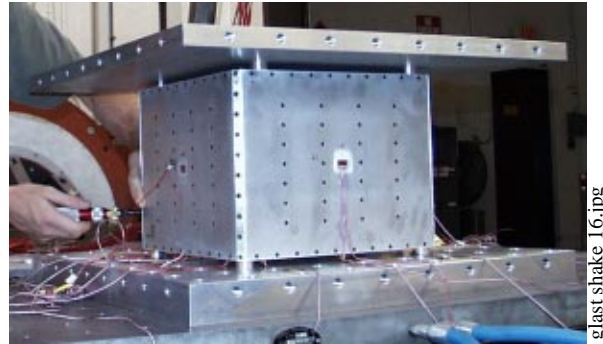


Figure 5-2. Illustration of the calorimeter mounted between the upper and lower test fixture mounting plates. The upper and lower mounting interface spacers are shown.

The two shear plates (small) were positioned on the +Y and -Y sides. The fasteners were engaged (finger tight) in the top and bottom fixture plates, but were not tightened at this time. The two long shear plates were positioned on the +X and -X sides. The 3/8-16 and 1/4-20 fasteners were engaged (finger tight) to align the six fixture plates. The four shear plates were tightened at this time to an unspecified torque level to align the side plates with the top and bottom plates. These assembly steps are illustrated in Figure 5-3. The two long shear plates were later removed so the calorimeter could be prepared for transportation to NRL. Note that these fastener threads were NOT coated with Loctite™ to ensure easy removal during testing.

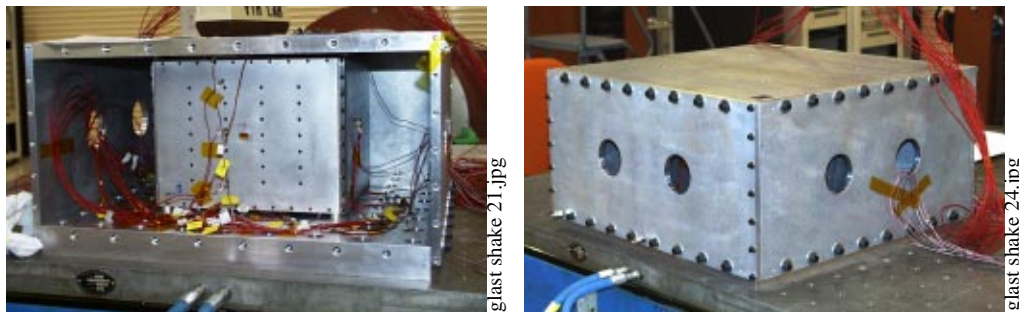


Figure 5-3. Illustration of the calorimeter mounted inside the test fixture. The calorimeter is shown with one long shear panel removed (left); and the test fixture completely enclosed (right).

Strain gage sensors were being monitored during the calorimeter/test fixture assembly to ensure that undue strains were not being introduced into the calorimeter during the assembly process.

5.3 Test Fixture/Shaker Table Mounting

The test fixture/calorimeter was mounted to each shaker using 56, 3/8" x 1.5", fasteners. The shaker table bolt patterns are similar for both the horizontal and vertical shakers. The fasteners clearance holes are located on the fixture base plate, inside the test fixture. This is shown in Figure 5-4. Access to the fastener locations was obtained by removing the two long shear plates from the fixture. All four sides were removed during the transverse test set-up to help make the fixture mounting easier. All 56 fasteners were torqued to 350 in-lbs to ensure proper pressure is maintained during testing. This torque requirement was provided by NRL-SVTF.

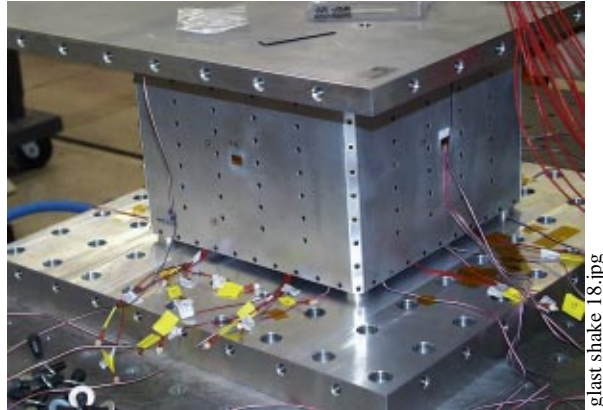


Figure 5-4. Fastener locations for Test Fixture/Shaker Table mounting.

The shaker that was being used for each test dictated the location of the test fixture/calorimeter assembly. The transverse axis tests used the horizontal shaker, which had a rather large table available. The test fixture was mounted to the shaker table near one edge, but centered along the excitation axis. This allowed easier access to the calorimeter while setting up instrumentation and mounting. The thrust axis test used the vertical shaker. The test fixture/calorimeter assembly was mounted in the center of the table, which was also the center of excitation. Figure 5-5 shows the test fixture/calorimeter mounting locations used for both the transverse and thrust axis tests.

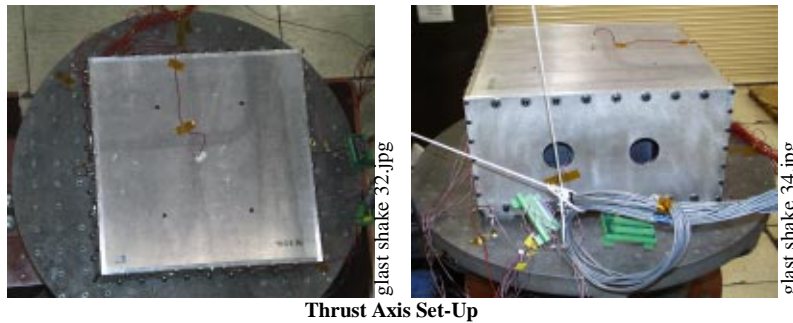
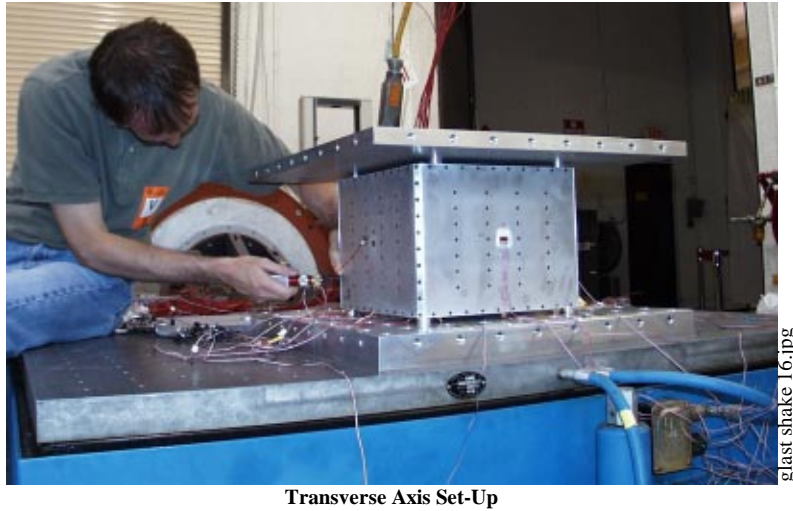


Figure 5-5. Test Fixture/Calorimeter mounting location for the transverse axis test (top) and the thrust axis test (bottom).

6. Signature Test Levels

A low-level random vibration test replaced the sine sweep test to characterize the calorimeter response and identify damage that may occur during the vibration testing. A low-level input is desirable to keep the structural response to a minimum, however the signal/noise ratio must be high enough to capture the characteristic response of the structure between 20 and 2000 Hz with a high degree of confidence.

The low-level random vibration test was defined using a band-limited white noise spectrum between 20 and 2000 Hz. The power spectral density (PSD) level is $0.0001 \text{ g}^2/\text{Hz}$ and the total acceleration is $0.45 \text{ g}_{\text{rms}}$. Figure 6-1 illustrates the actual input spectrum measured during low-level random vibration testing for the two input control channels. The input spectrum was notched around one of the shaker frequencies at $\sim 1300 \text{ Hz}$. This is a compression mode of the shaker table and causes severe oscillations and separation between the shaker table and the test article.

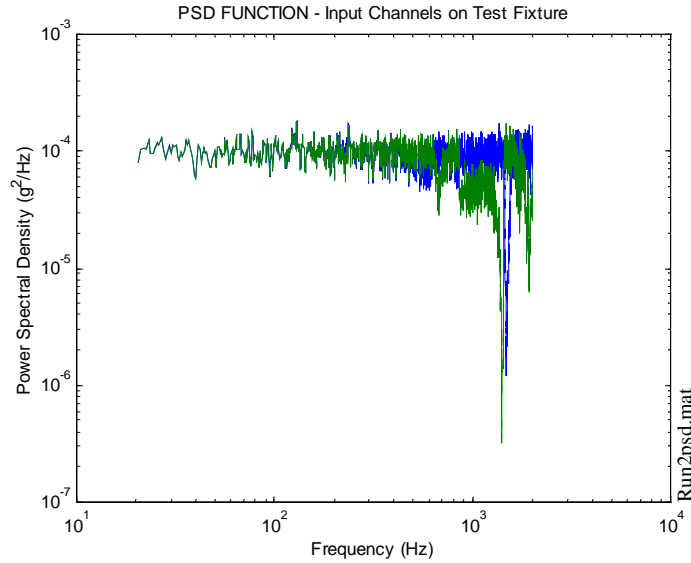


Figure 6-1. Measured input spectrum for the two input control channels.

7. Sine Burst Test Levels

7.1 Input Test Level Defined in Test Plan

The Shake Test 99 calorimeter will be subjected to a qualification level sine burst test to validate the design concept to the launch environment and qualify the workmanship. The sine burst test is designed to subject the calorimeter to the quasi-static limit load factors used in the design analysis. The limit load factors are defined in the GLAST Science Instrument – Spacecraft Interface Requirements Document (SI-SC IRD), paragraph 3.2.2.7.2.

The acceleration levels used for the qualification level sine burst test are defined by adding 25% to the limit load factors defined in the SI-SC IRD. The limit loads are given to be $\pm 4.0 g's_{0-pk}$ in the lateral direction during liftoff and transonic events, and $\pm 6.6 g's_{0-pk}$ axially during main engine cutoff. The acceleration levels for the qualification level sine burst test are calculated to be $\pm 5.0 g's_{0-pk}$ in the transverse direction and $\pm 8.25 g's_{0-pk}$ in the thrust direction.

The acceleration levels have been defined, but an acceptable frequency must be calculated. Because this is a quasi-static test, the frequency used for the sine burst test must be low enough to avoid structural resonance of any part of the structure. Resonance would cause large deflections and possible damage to the calorimeter. The deflection amplitude of the shaker will dictate the sine dwell frequency. The dwell frequency is inversely proportional to the amplitude; therefore the largest obtainable amplitude will be used to define the dwell frequency. The vertical and horizontal shakers were believed to have a maximum range of 1" (0.025 m) pk-pk. The sine burst dwell frequency was calculated using the following equation:

$$a = [A (2 \cdot \pi \cdot f)^2] / 9.81 \tag{7.1}$$

Here,

- a = base acceleration in g's,
- A = amplitude of base excitation in meters,
- f = dwell frequency in Hz.

Using the base acceleration levels and excitation amplitude outlined in the previous paragraph, the dwell frequency can be backed out of equation 7.1. The dwell frequency for the transverse axis test was calculated to be 9.9 Hz. The dwell frequency for the thrust axis test was calculated to be 12.7 Hz. Table 7-1 summarizes the defined sine burst test levels for both test axes.

Table 7-1. Defined Sine Burst Test Levels

Test Axis	Dwell Frequency	Acceleration Level	Duration
Transverse	9.9 Hz	±5.0 g's _{0-pk}	5 cycles
Thrust	12.7 Hz	±8.25 g's _{0-pk}	5 cycles

7.2 Input Test Level Used

The sine burst test levels defined in section 7.1 had to be adjusted slightly. The maximum amplitude was assumed to be 1" pk-pk, which was correct, however the shaker could not achieve this theoretical value exactly at the frequency defined; there would be some overshoot which would exceed the maximum allowable amplitude. Therefore, the sine burst deflection amplitude was reduced, allowing the dwell frequency to increase. The dwell frequency was selected to be 12 Hz for the transverse test and 15 Hz for the thrust test. Both values were substantially lower than the estimated fundamental frequency of the calorimeter, eliminating any risk of damage due to structural resonance of the calorimeter.

Limitations of the shakers kept the tests from being performed as theoretically described in section 7.1 (i.e. 5 cycles of constant amplitude excitation). The shakers required both a ramp-up and a ramp-down to achieve the desired excitation amplitude. To accommodate this requirement, a modified but equivalent input time history function was used. This function can be described as a constant frequency excitation at the prescribed dwell frequency, where the amplitude is varied according to a ½ sine envelope. The input functions used for both the transverse and thrust axis tests are illustrated in Figure 7-1 (note the variable amplitude). Two input control channels were used during the testing and are both shown in this Figure.

Quickly, one can identify that by using the functions illustrated in Figure 7-1, five complete cycles at the full amplitude are not achieved. However, the use of this input time history function can be justified because at least 4 cycles will be executed at > 94% of the maximum amplitude, two of which will exceed > 99%. In addition, five cycles was an arbitrary number that was selected because it was believed to give a good statistical population of the expected calorimeter response to the input sine burst.

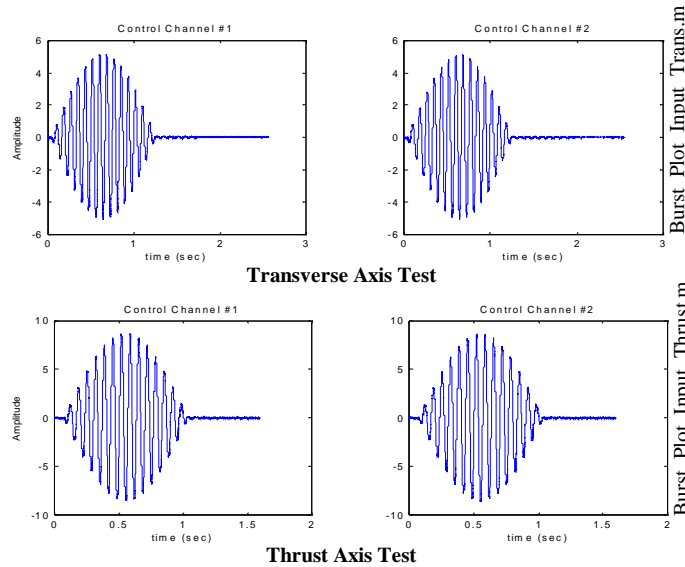


Figure 7-1. Illustration of the experimental input levels used for the sine burst tests. The dwell frequency was 12 Hz for the transverse test (top) and 15 Hz for the thrust test (bottom). The amplitude is given in g's.

8. GEVS Specified Random Vibration Test Levels

8.1 Full Amplitude Random Vibration Test Level Defined in Test Plan

The Shake Test 99 calorimeter random vibration test levels are specified in the GEVS, section 2.4 – “Structural and Mechanical”, paragraph 2.4.2.5 – “Component/Unit Vibroacoustic Tests”, sub-paragraph (a) – “Random Vibration.” This paragraph outlines that the test component (calorimeter) shall be subjected to a random vibration along each of three mutually perpendicular axes for one minute each. When possible, the random vibration spectrum shall be based on levels measured at the mounting locations during previous testing. The second alternative is to use a statistically estimated response of similar components mounted on similar structures or on analysis of the payload. The Generalized Vibration Test Specification of Table 2.4-4 is used when previous measurements of similar structures and analytical solutions are not available.

GEVS Table 2.4-4 was used to determine the test levels for the Shake Test 99 calorimeter testing because response data from similar structures and analyses are not available. The table gives exact qualification and acceptance level Acceleration Spectral Density (ASD) functions, given in g^2/Hz , for components weighing 22.7 kg. Qualification levels are defined as the flight limit level, acceptance, plus 3 dB. The table also specifies that the ASD levels may be reduced for components weighing more than 22.7 kg, and must adhere to the following equations for qualification level vibration tests:

$$\text{DB Reduction} = 10 \log(W_1 / 22.7) \qquad 10 \log(W_2 / 50) \qquad (8.1)$$

$$\text{ASD}(50\text{-}800 \text{ Hz}) = 0.16 (22.7 / W_1) \qquad 0.16 (50 / W_2) \qquad (8.2)$$

Where,

W_1 = Component Weight in kg.

W_2 = Component Weight in Lbs.

The minimum ASD level must be maintained at $0.01 \text{ g}^2/\text{Hz}$ at 20 and 2000 Hz for components that weight more than 59 kg and the slope from 20 to 50 Hz and 800 to 2000 Hz, shall be adjusted to maintain these levels.

The actual Acceleration Spectral Density levels that were used in the random vibration test of the Shake Test 99 calorimeter are listed in Table 8-1. Figure 8-1 illustrates the ASD levels for the vibration tests and indicates the maximum and minimum values outlined in the GEVS. The actual ASD levels used for the random vibration test were calculated using the actual Shake Test 99 calorimeter weight of 111.4 kg (245 lbs). This weight was measured prior to installation inside the test fixture.

Table 8-1. Acceleration Spectral Density Levels for the Random Vibration Test.

Frequency (Hz)	ASD Level (g^2/Hz)
20	0.01
20 to 50	+3.92 dB/oct
50 to 800	0.033
800 to 2000	-3.92 dB/oct
2000	0.01
6.81 grms	

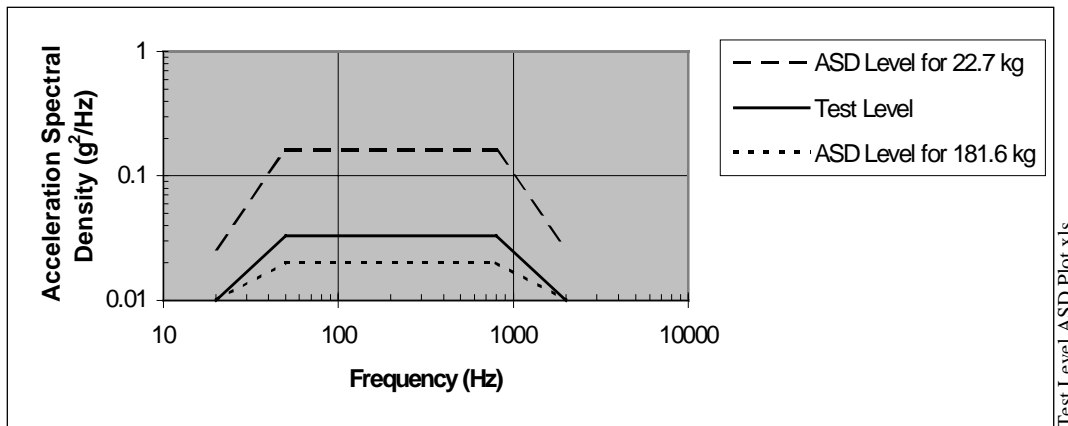


Figure 8-1. Generalized Random Vibration Test Levels for the Shake Test 99 Calorimeter.

The GEVS also allows these levels to be notched around fundamental modes of delicate equipment such as the CsI calorimeter, when damage to the hardware is likely to occur. Both tests will be stepped up to avoid damage to the calorimeter. Tests were scheduled to subject each axis to a random vibration at $-6 \text{ dB} * 6.81 \text{ g}_{\text{rms}}$, at $6.81 \text{ g}_{\text{rms}}$ with

notch filtering, and finally at 6.81 g_{rms} without notch filtering. This allowed the calorimeter performance to be monitored at various levels of random vibrations.

8.2 Full Amplitude Random Vibration Test Level Used

The full amplitude random vibration tests used the input PSD defined by the GEVS in section 8.1. Two-channel maximum control was used to limit the input and was controlled using a Spectral Dynamics 2550B control system. NASA requires that the input level be controlled to ± 3 dB. The control resolution was 5 Hz or 400 lines between 20 and 2000 Hz. The control resolution defines how well the input spectrum is limited. An increase in resolution improves the control over the entire spectrum, but time is severely sacrificed. Both the line tolerance and overall tolerance were set to ± 1.5 dB.

Figure 8-2 is a plot of the two input control channels. The GEVS specified ASD function, along with the two ± 3 dB limits, is shown as a reference. The mean control signal is within tolerance for all frequencies, however local minima begin to drop below the -3 dB limit above 600 Hz. Control channel #1 drops below the lower limit once around 600 Hz and not again until ~ 1300 Hz. Control channel #2 drops to the -3 dB limit and was held there for frequencies above 600 Hz.

The variations that occur around and above 600 Hz are unknown, however it is worth noting that they coincide with the natural frequencies of the test fixture (~ 600 Hz and above). The notch near 1300 Hz is due to the controller's response to a shaker table resonance at that frequency. This is a compression mode of the slip table.

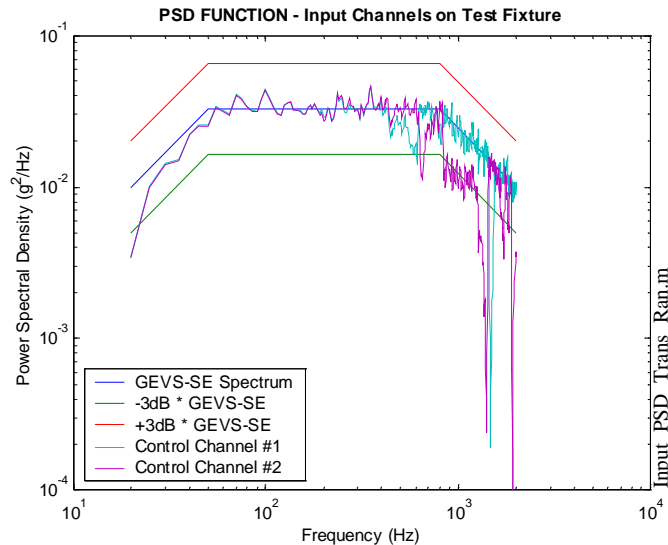


Figure 8-2. Input spectrum for the full amplitude random vibration tests. The two control channels are shown along with the GEVS-SE specified spectrum and ± 3 dB Limits.

9. Instrumentation

9.1 Accelerometers

9.1.1 Types

The SVTF had a number of accelerometers available for the random vibration tests. Four different accelerometers were used throughout the testing for both test axes. The accelerometers were all piezoelectric, manufactured by ENDEVCO. Table 9-1 lists the different accelerometers used during testing along with a general description and quantity used.

Table 9-1. ENDEVCO accelerometers used during vibration testing.

Model	Description	Qty
7702A-50	Stud Mounted, general vibration measurement, piezoelectric accelerometer	2
2222C	Sub-miniature, general vibration measurement, piezoelectric accelerometer	25
2226C	Miniature, general vibration measurement, piezoelectric accelerometer	2
2229C	Miniature, general vibration measurement, piezoelectric accelerometer	4

The 2222C accelerometers are very small and lightweight, which make them ideal for measuring the calorimeter response. Clearance limitations prohibit the use of large accelerometers, which may have also caused an increase in the modal mass, thereby lowering the natural frequencies. For this reason, all 25 2222C accelerometers were mounted on the calorimeter. The two 7702A-50 accelerometers were used to measure the input signal and the remaining 2226C and 2229C accelerometers were used to measure the test fixture response.

9.1.2 Mounting Locations

9.1.2.1 Transverse Axis Testing

The test fixture/calorimeter was instrumented with 33 accelerometers. Many of these measurements were redundant, but later proved to be necessary when several accelerometers fell off during testing. The specific accelerometer mounting locations are listed in Appendix B, for reference.

The calorimeter was instrumented with 25 accelerometers. The primary objective was to capture the response of the CsI logs due to lateral forces, and measure their interaction with the containment /shear panel assembly. Additional accelerometers were required to understand how the structural response is coupled with the two orthogonal directions.

The CsI logs were instrumented with eight accelerometer on the +X side to measure the response of each row in the x direction. The +Y side was instrumented with four accelerometers. Two accelerometers were used to measure the response in the x direction and the remaining two were used to measure the response in the y direction. Figure 9-1 shows the accelerometer mounting locations used to measure the CsI log response. Locations 10 and 13 were used to measure the response in the y direction.

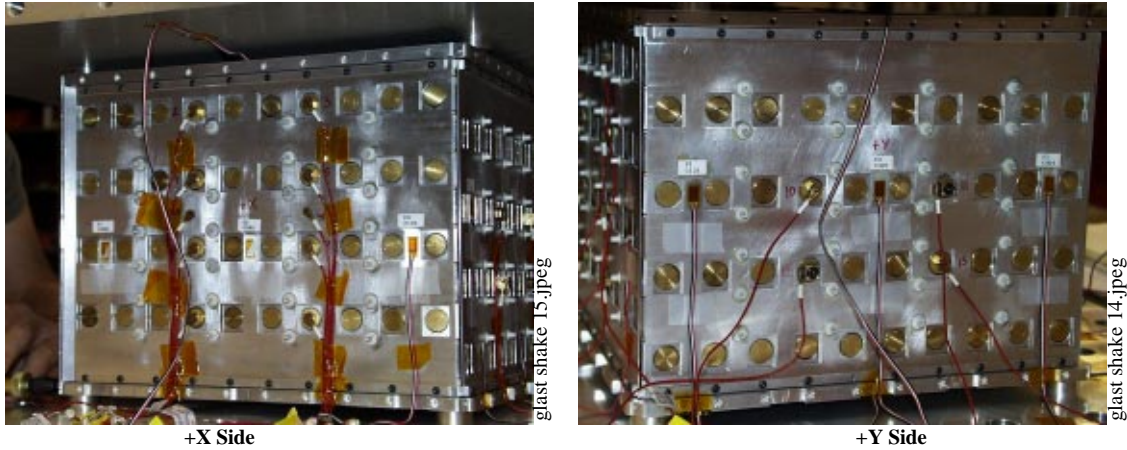


Figure 9-1. Illustration of the accelerometers mounted to the CsI log. The eight locations are shown on the +X side (Right) and the four locations are shown on the +Y side (Left). Locations 10 and 13 were used to measure the response in the y direction on the +Y side.

The remaining accelerometers were used to monitor the response of the remaining panels. The top compression panel was instrumented with one accelerometer to capture the vertical motions and panel modes. The accelerometer was centered along one edge and placed away from the edge (towards the center) to capture the response of the panel. This location was not critical, therefore only one accelerometer was used.

The +X side containment panel was instrumented with two accelerometers to help capture the coupled response between the CsI logs, the containment panels and the shear panels. These accelerometers can also be seen in Figure 9.1.2.1-1, on the +X side. They are located between the two middle rows of CsI logs.

The shear panels were instrumented with accelerometers on all four sides. The +X side was instrumented with three accelerometers: one on the top, one in the middle and the third at the bottom of the panel. These accelerometers were intended to capture both the frequency and mode shape of the containment/shear panel assembly. The remaining sides were instrumented with accelerometers in the middle of the panel to measure the frequency only. The $\pm Y$ sides were instrumented with tri-axial accelerometers (three 2222C type accelerometers mounted to one tri-axial mounting block) to measure the response in the y & z directions in addition to the x direction. Figure 9-2 shows the mounting locations used for the +X side and the tri-axial mounting on the +Y side.

The test fixture was instrumented with accelerometers on the +X, +Y and +Z sides. Figure 9-3 shows the test fixture instrumentation. Five accelerometers were used to measure the test fixture response in the x direction on the +X side. The two accelerometers on the bottom of the test fixture were used as the control channels to monitor and limit the input signal. The +Y side was instrumented with two accelerometers. The top accelerometer will capture any shear modes. Panel modes in the y direction were not of interest. The top panel was instrumented with one accelerometer to measure the response in the z direction, as well as measure the panel modes. The coupling between the test fixture panel modes and the calorimeter was of particular interest during thrust direction tests.

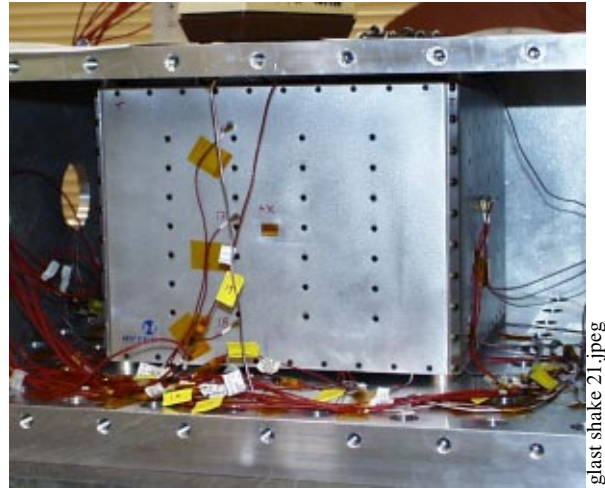


Figure 9-2. Illustration of the accelerometer mounting locations used for the calorimeter shear panels. The +X side is shown.

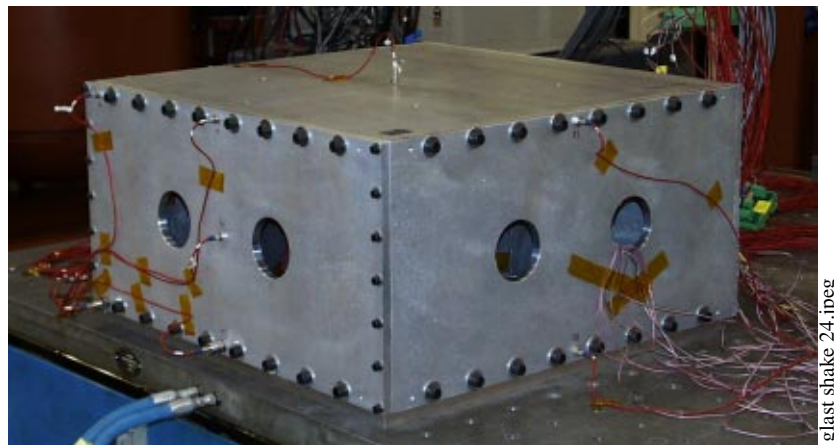
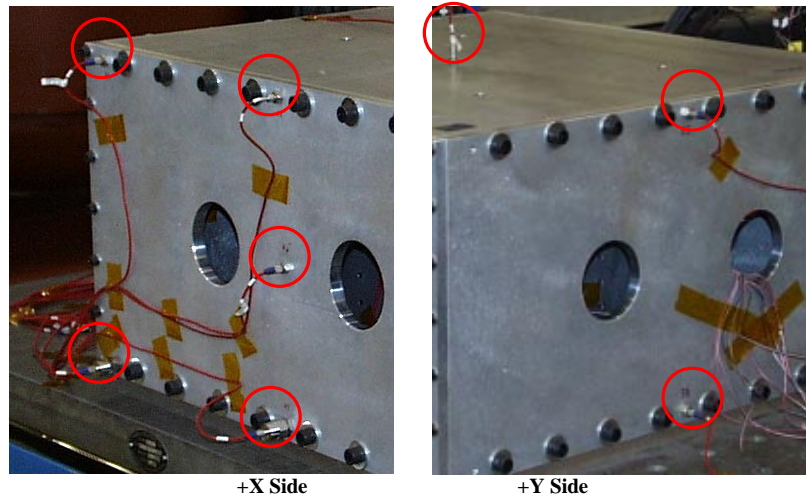


Figure 9-3. Illustration of the test fixture accelerometer mounting locations (Bottom). The top pictures are enlargements of the mounting locations on the +X (Top Left) and +Y (Top Right) sides, respectively. Accelerometers are circled for clarity.

9.1.2.2 Thrust Axis Testing

The instrumentation for the thrust axis testing did not require much modification from the transverse axis tests. All of the accelerometers remained in their respective positions and measured the same directions as with the transverse tests, with the exception of the eight accelerometers mounted on the CsI logs on the +X side and the control channel accelerometers. The eight accelerometers on the +X side were reoriented to measure the response of the CsI logs in the vertical direction. Figure 9-4 illustrates the mounting configuration. Notice that the accelerometer mounting block #2 was replaced with accelerometer mounting block #1 to mount the accelerometers in the vertical direction. The two control channel accelerometers had to be moved to the shaker table to measure the input signal in the vertical direction. Mounting the control channels to the test fixture would have measure the input signal in addition to the test fixture response.



Figure 9-4. Illustration of the accelerometer mounting locations on the +X side for the thrust axis tests. The accelerometers are oriented to measure the response in the z direction.

9.2 Strain Gage Sensors

The calorimeter has been instrumented with strain gage sensors to measure the static relaxation of the calorimeter after the initial compression. The sensors were available during the vibration testing; therefore they were used to measure the real time strains.

9.2.1 Types

The calorimeter was instrumented at HYTEC Inc. with 20 strain gage sensors manufactured by Vishay Measurement Group, Micro-Measurement Division. Two types of sensors were used and bonded to the containment panels, compression panels and shear panels. All of the sensor locations are listed in appendix C along with the type, location and axis direction. There are two different types of strain gage sensors, both of which are general purpose strain gages for static and dynamic stress analysis. The first used is the CEA-13-250UW-120 which is a single element (axis) sensor, and the second is the CEA-13-250UR-120 which is a three element rosette sensor. The following will help understand the strain gage designation just identified:

- CE – Flexible gages with a cast polyimide backing and encapsulation featuring large, rugged, copper-coated solder tabs. This construction provides optimum capability for direct leadwire attachment.
- A – Constantan alloy in self-temperature-compensated form.
- 13 – The approximate thermal expansion coefficient in ppm/°F on the structural material on which the gage is to be used.
- 250 – Active Gage Length in Mils (0.001 in)
- UW,UR – Grid and Tab Geometry
- 120 – Resistance in Ohms

9.2.2 Mounting Locations

Each containment panel was instrumented with three single element strain gage sensors at the mid-plane of the panel. One sensor each was spread across the panel; one on the left edge, one at the center and the third on the right edge. This is illustrated in Figure 9-5. The sensors were bonded to the containment panel to measure the in-plane strain due to lateral forces, and oriented to measure the vertical strain in the z direction.

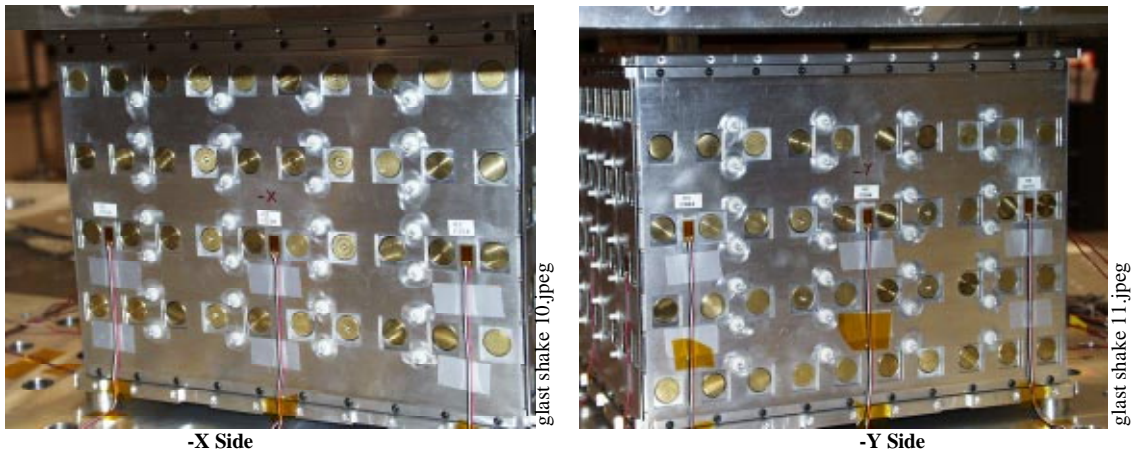


Figure 9-5. Illustration of the strain gage sensor locations bonded to the containment panels. The -X (Left) and -Y (Right) sides are shown.

The top and bottom compression panels have been instrumented with two strain gage sensors each at the center of the panel. They are single axis gages oriented to measure the strain along both the x and y axes(one each).

The shear panels have been instrumented with strain rosettes to measure the in-plane strain due to lateral forces. Each shear panel has one rosette bonded at the center of the panel that is oriented to measure the strain in the z direction as well as the off-axis strain, $\pm 45^\circ$ from vertical. This is illustrated in Figure 9-6. The strain measurements for the $\pm X$ shear panels were not recorded because the stresses are mostly due to out-of-plane bending from the lateral motions. The shear in the $\pm Y$ panels was of the greatest concern and therefore measured. The stresses found in the two Y panels are mostly due to in-plane shear caused by lateral motions. The leadwire for the $\pm Y$ panels can be seen in Figure 9-6, whereas there is no leadwire for the $\pm X$ panels.

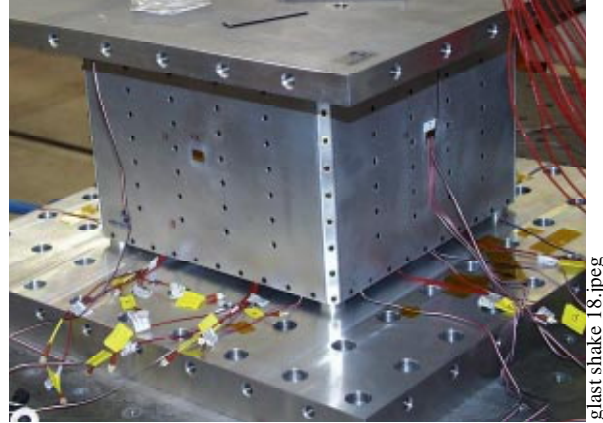


Figure 9-6. Illustration of the strain gage sensors bonded to the shear panels. Note that the +X rosette was not wired for measurement.

10. Test Plan Summary

A test plan was written, “GLAST Shake Test 99 Calorimeter Random Vibration Test Plan”^[4], to organize the vibration tests for the Shake Test 99 Calorimeter. The plan called for three types of tests to be performed on two of the three orthogonal axes; parallel to one of the transverse axes (horizontal) and parallel to the thrust axis (vertical). The third axis did not need to be tested due to symmetry of the calorimeter.

Three types of tests were planned. The first was a low amplitude signature characterization of the calorimeter FRF’s. A sine sweep test was planned, however a low level random vibration test was performed in its place. The second test was a sine burst to validate the design to the equivalent quasi-static limit loads. The third was the qualification level random vibration test to validate workmanship and survivability to the harsh launch environment.

The test plan outlined a test sequence to perform each of the required tests. The planned test sequence and actual test sequence are recorded in Appendix A of this report. Section 13.1 summarizes the test sequence as performed parallel to the transverse axis and section 13.2 summarizes the test sequence as performed parallel to the thrust axis. In summary, both test axes were subjected to the following tests, in the order shown.

1. A low amplitude random vibration test was performed to get a signature characterization of the calorimeter.
2. A sine burst test was performed at $\frac{1}{2}$ the acceleration levels.
3. A random vibration test was performed at -6 dB * Full Amplitude.
4. Another low amplitude random vibration test was performed to verify no damage has occurred during the two previous tests.
5. The full amplitude sine burst test was performed to qualify the design under quasi-static loading.
6. Another low amplitude random vibration test was performed to verify no damage has occurred during the full amplitude sine burst test.
7. The qualification level full amplitude random vibration test was performed. Notching was eliminated from this test because of the low Q of the dominant modes.
8. Another low amplitude random vibration test was performed to verify no damage has occurred during the full amplitude random vibration test.

The calorimeter was moved to the vertical axis shaker and the tests were repeated parallel to the thrust axis.

11. Vibration Test Results

This section describes the series of vibration tests performed on the calorimeter to validate the mechanical design. Experimental measurements are described and discussed, and post-processing of the transfer functions are performed to identify unknown properties such as natural frequencies, mode shapes, damping ratios and quality factors.

11.1 Transverse Axis Test Results

11.1.1 Random Vibration Test

The Shake Test 99 calorimeter was subjected to three levels of random vibration in the transverse direction as described in Sections 6 & 8. During these tests, the experimental transfer functions were recorded using an FFT analyzer. The results from the transverse axis test are described herein.

One of the test objectives was to determine the response of the CsI logs and ensure that they are not striking the containment/shear panel during launch. This could damage the logs and make them inoperable. Lumped parameter analysis predicted that the logs would not strike the containment panels. Experimental tests confirmed this with the latest calorimeter design.

Another goal of the test was to determine the fundamental frequency of the CsI stack so that the FE models could be updated. The horizontal transfer functions between the base and the CsI logs are compared in Figure 11-1. Notice that only six of the ten accelerometer locations are shown on this plot. To avoid showing too much data, only one transfer function is shown for each row of CsI logs, where available. The plot shows that the fundamental frequency is slightly greater than 90 Hz (~91 Hz). Several additional modes can be seen above 600 Hz, however the spectral content is very dense, making it difficult to clearly identify those modes. The dense spectral content can be attributed to test fixture modes that were expected at frequencies above 600 Hz (the fundamental test fixture mode occurs at ~600 Hz), and the addition of shaker modes that appear at even higher frequencies (> 1000 Hz).

From this plot some sense of the mode shape can be envisioned. The boundary conditions are such that the calorimeter is fixed at four locations on the top and bottom compression panels. Therefore, the expected mode shape of the fundamental transverse mode would be a $\frac{1}{2}$ sine wave deflection envelope of the CsI layers, with the center logs having the greatest motion. Using this assumption, one would expect the center logs to have the greatest accelerations with the acceleration magnitude decreasing as a sinusoid near the outer edges. Examination of the transfer function shows that the 1st row has the smallest amplitude and the center logs have the largest.

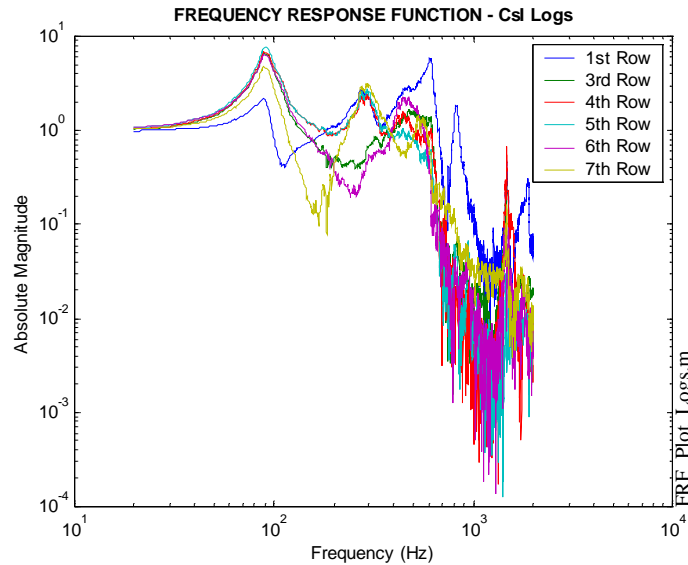


Figure 11-1. Plot of the horizontal transverse transfer functions for the base to six of the ten CsI logs.

A modal identification software package^[9] was used to help extract the natural frequencies, mode shapes, damping ratios and quality factors. The mode shapes of interest are the coupled motions of the CsI stack with the containment/shear panel assembly. Recall that the CsI logs are mechanically coupled with the containment/shear panels through a foam layer that was installed between the two, to help damp energy that would cause the CsI logs to strike one of the containment panels.

Eleven of the thirty-three measurement locations were used to identify the transverse mode shapes of the CsI stack. Four measurements from the +X side CsI logs, two measurements from the +Y side CsI logs, two measurements from the center of the containment panel, and three measurements from the +X shear panel were used. Figure 11-2 shows a comparison of the relative measured transfer function (blue) and the best-fit transfer function (green), obtained with the modal identification software, for the response of the CsI log on the bottom row. The estimated transfer function matches the experimental transfer function with a high degree of confidence for the fundamental mode, however the two higher modes are not estimated with nearly the same degree of confidence (although still quite good for the CsI stack measurements). This will be reflected in the mode shape identification, but the results will still provide some insight into understanding the response of the calorimeter during launch. Plots similar to that shown in Figure 11-2 for all eleven channels used in the modal identification are shown in Appendix D. One can see that the higher frequency response for the containment panels (channels 10 & 11) and shear panels (channels 7, 8 & 9) is very modally dense and will be difficult to estimate the mode shape response at these locations.

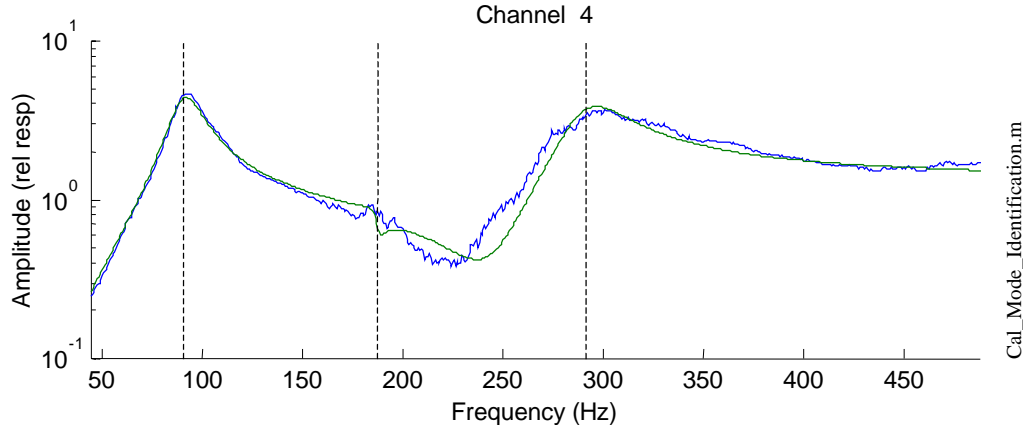


Figure 11-2. Plot showing the experimental transfer function (blue) and the estimated transfer function (green) used in the modal identification. The dashed vertical lines represent the estimated natural frequency poles.

The results of the modal identification analysis revealed the first three transverse modes. The natural frequencies (f), damping ratios (ζ) and quality factors (Q) are given in Table 11-1 and are compared to the simulation results from the MATLAB model (lumped mass). The quality factor is the inverse of twice the damping ratio.

$$Q = 1/(2 \zeta) \quad (11.1)$$

Table 11-1. Dynamic properties identified from the experimental results and compared to the MATLAB model simulations.

Mode	MATLAB	Experimental		
	Frequency	Frequency	Damping Ratio	Quality Factor
1 st Transverse Shear	88.1 Hz	91 Hz	9.3%	5.4
2 nd Transverse Shear	172.5 Hz	187 Hz	1.9%	26.3
3 rd Transverse Shear	251.2 Hz	292 Hz	6.1%	8.2

There is a high degree of confidence that all three frequencies have been identified accurately, and there is good correlation with the MATLAB results. The second mode is less obvious from the experimental data, however the MATLAB results confirm it has been properly identified. There is also a high degree of confidence that the damping ratio for the 1st mode is accurate. The confidence level drops off when looking at the 2nd and 3rd mode damping ratios. Poor correlation between the measured and best-fit transfer functions for the containment panels and shear panels is the cause of difficulty in accurately determining the structural damping for the higher modes. The plots in Appendix D, channels 7 thru 11, clearly illustrate this.

In addition to the dynamic properties, the modal identification analysis was able to identify the three mode shapes associated with the three frequency poles. The experimental mode shapes are shown in Figure 11-3 and compared to MATLAB predictions. The experimental mode shapes are shown on the left. The un-deformed shape is shown as a dashed line for reference, where the left line represents the CsI stack and the right line represents the containment/shear panel assembly (both on the +X side).

There is clearly excellent agreement for the 1st and 3rd frequency mode shapes between the experimental results and MATLAB predictions. The 2nd frequency mode shape doesn't appear to represent the expected response as predicted by MATLAB. This is due to the difficulty in estimating the frequency pole at the second peak.

To better understand how the CsI logs are coupled with the containment/shear panel assembly, Figure 11-4 was plotted to show that the transfer functions for the containment/shear panel assembly are similar to that of the CsI stack for the fundamental mode. The amplitude is reduced which indicates a good agreement with the 1st transverse mode shape identified in Figure 11-3, where the deflection amplitude is clearly smaller. Higher frequencies become lost in the modally dense response of the containment/shear panel assembly.

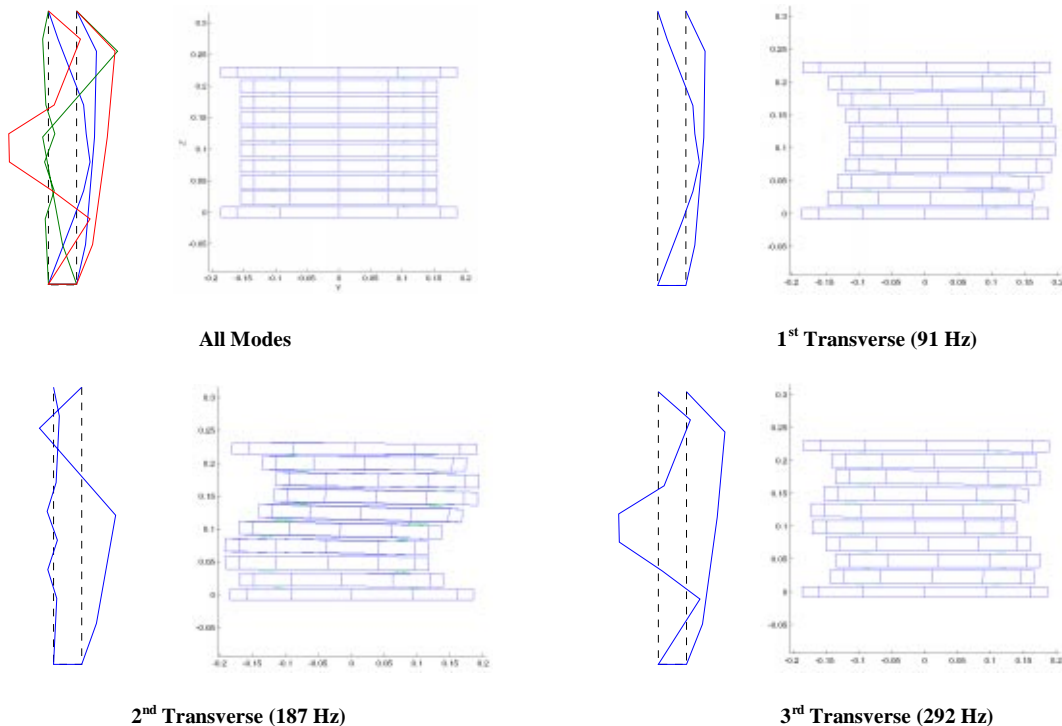


Figure 11-3. Illustration of the first three CsI stack/containment panel/shear panel modes. The experimental mode shapes (left) calculated from the measured transfer functions are shown and compared to the MATLAB predictions (right).

During the modal analysis, the response of the CsI stack was shown to be amplitude dependent. Figure 11-5 plots the horizontal transfer function between the base and one center CsI log for all of the random vibration tests performed. This includes the four low-level random signature characterizations, the -6 dB random and the full amplitude random. It is shown that as the input acceleration levels increase, the natural frequency and quality factors decrease, while the damping ratio increases. The increased damping ratio is identified by the decrease in amplitude and an increase in the 1/2-amplitude bandwidth. The fundamental frequency dropped from ~110 Hz for the low level random, to ~100 Hz for the -6 dB random and finally to 91 HZ for the full amplitude random.

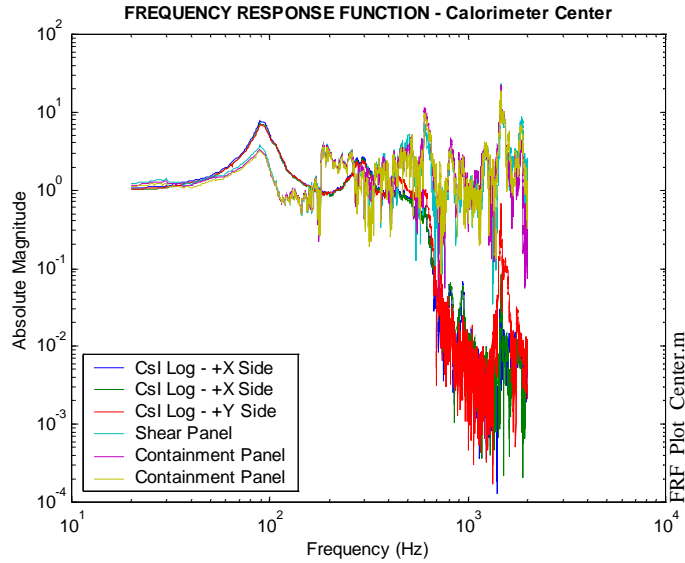


Figure 11-4. Plot of the horizontal transfer function for three of the CsI logs, the shear panel and containment panel.

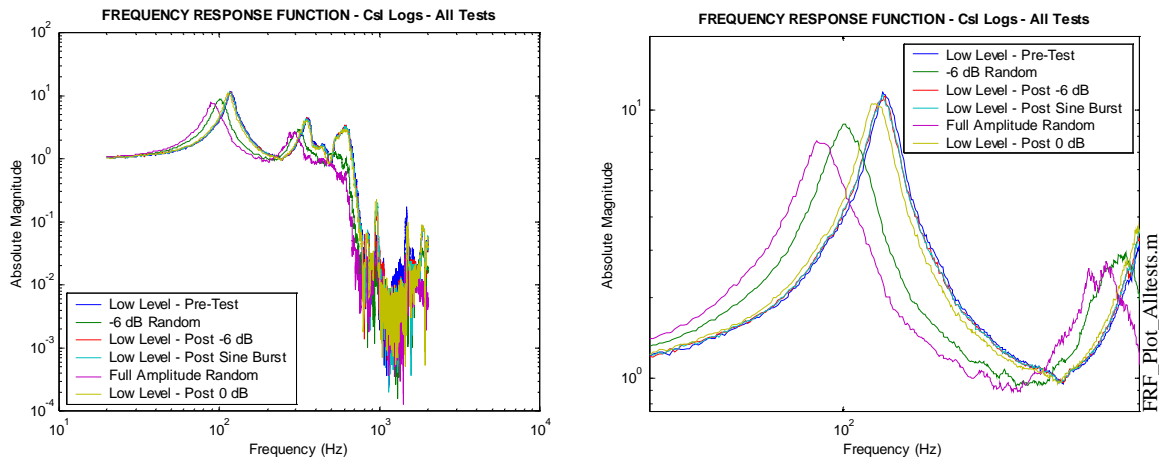


Figure 11-5. Plot of the horizontal transfer function for all six random vibration tests (left). The transfer function is from the base to the CsI log located at the center of the calorimeter. A blowup of the fundamental peak is illustrated for clarity (right).

This amplitude dependence for both frequency and quality factor of the CsI stack was expected. Typical rubber compounds are known to exhibit nonlinear stiffness characteristics demonstrated in these tests. Similar characteristics were also observed in an earlier random vibration test performed on three CsI logs sandwiched between two layers of a similar rubber compound.

This dependence is caused by the materials dynamic properties. Rubber is a non-compressible compound with viscoelastic properties. The dynamic modulus (a term used to indicate the mean stress-strain ratio of dynamic stress caused by oscillations greater than 0.1 Hz) is known to be dependent on both the base excitation frequency (strain-rate) and amplitude of deformation (max-strain), as described in [5]. The base excitation frequency only affects the dynamic modulus at frequencies below 20 Hz and above 10^6

Hz; everything between remains relatively constant. For this reason, the amplitude dependence identified in these tests is a result of changes in the amplitude of deformation. The dynamic modulus decreases by as much as 25% in the first 2.5% strain as the excitation amplitude increases; this agrees with the stack response in Figure 11-4.

11.1.2 Sine Burst Test

The goal of the sine burst test was to validate the design and workmanship to the static limit load factors used in the design analyses. The sine burst test subjected the calorimeter to a quasi-static qualification level acceleration of 5 g's at 12 Hz. The time history acceleration and strain response was recorded for analysis.

It is difficult to draw many conclusions from the acceleration time history data other than the design and workmanship has successfully withstood the qualification level sine burst test along the transverse axis. The calorimeter can be expected to survive the static equivalent launch environment without damage. Post-test inspection and a low-level random vibration characterization (before and after the sine burst test), confirm that there was no damage during testing. Figure 11-6 is a plot of the low-level random vibration characterization that was performed before all testing, after the 1/2 amplitude sine burst test and again after the full amplitude sine burst test.

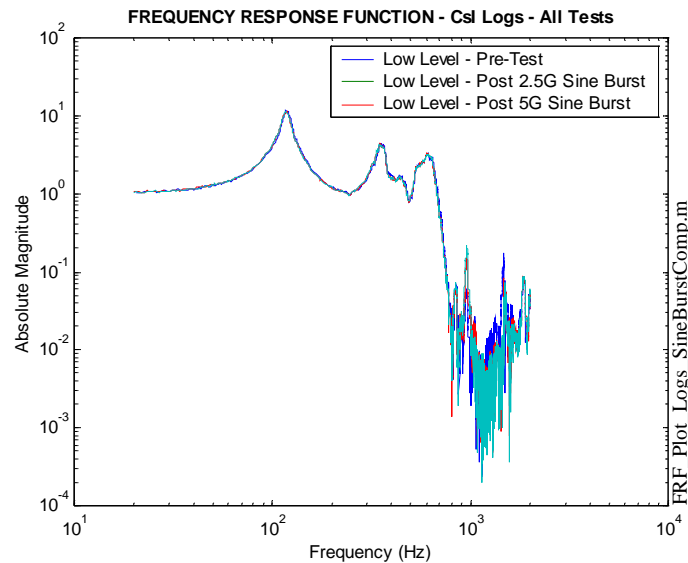


Figure 11-6. Plot of the horizontal transfer function for the three low-level random vibration characterization tests performed before all tests, after the 1/2 amplitude sine burst test and again after the full amplitude sine burst test.

The sine burst test can also be used to detect slippage between the CsI logs and the rubber layers. Earlier tests demonstrated that the response time history curve of the CsI logs would look like a square waveform if slippage occurs. When plotted against the base acceleration time history, the curves are in-phase with one another tracing the sinusoidal waveform until the separation acceleration was reached. At this time, friction would be overcome and the response acceleration would cease to increase.

The response of the CsI stack was examined for separation. Figure 11-7 shows the response of a single log for each row in the stack. The time history response is plotted for each location and the base acceleration is shown for reference. Magnification of the maximum amplitude peaks is shown for clarity. Examination of these plots reveals that no slippage has occurred during the sine burst test. The preload has been adequately defined.

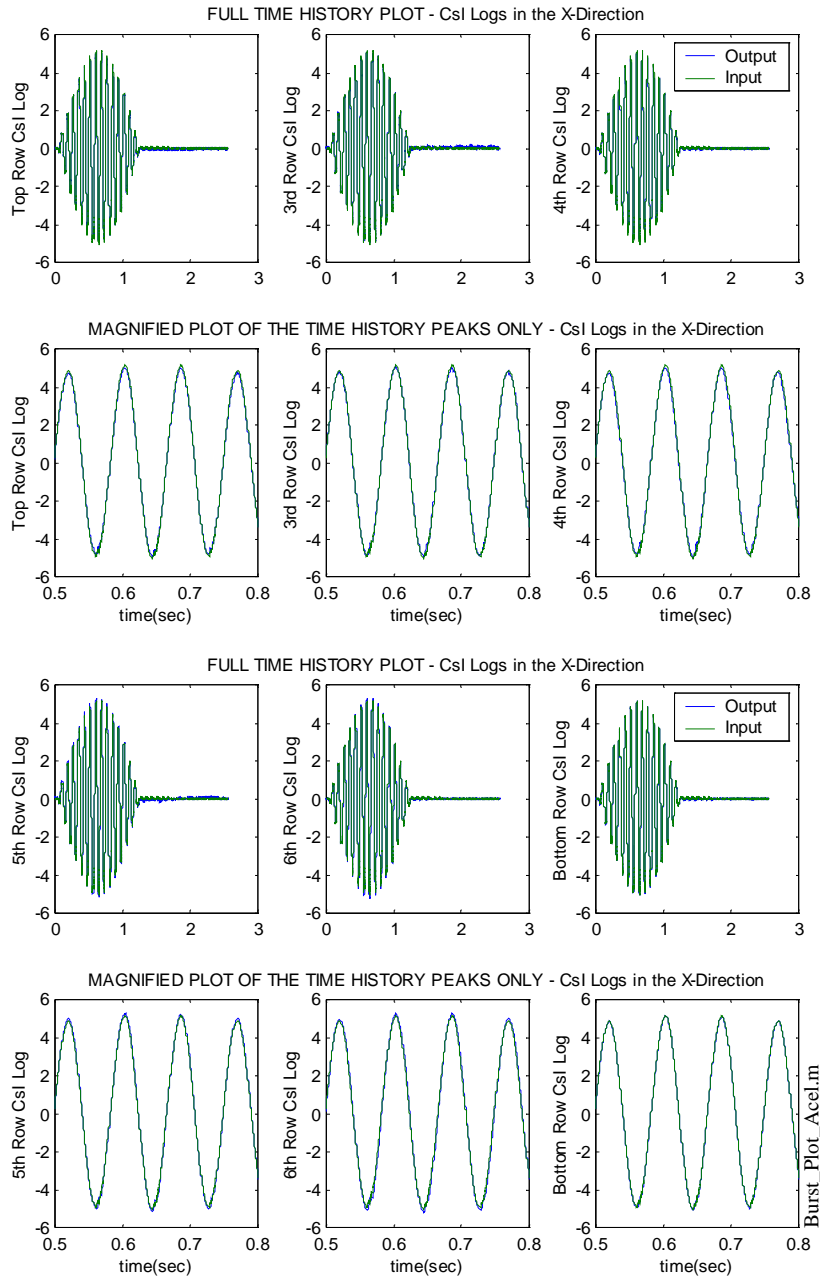


Figure 11-7. Acceleration time history response (blue), in g's, for one CsI log on each row. Magnification of the time history is show for clarity and the base acceleration (green) is shown for reference.

Strain measurements were also recorded during the transverse sine burst test. One goal of taking the strain measurements was to measure the shear strain in the shear panels and compute the in-plane principal and shear stresses. Each of the four shear panels was instrumented with a single strain rosette. The response of the two Y side panels was recorded and the stresses were computed. Additional strain measurements were taken on the containment panels, however limited information about the stress-state was known and the in-plane stresses could not be accurately computed.

Figure 11-8 shows the shear panel strain measurements recorded during the full amplitude sine burst test (additional strain measurements are shown in Appendix E). The top three plots are the strain measurements for the +Y side and the bottom three plots are the strain measurements for the -Y side. The -Y side response illustrates the expected response of a panel subjected to shear deformations. The two outside elements are symmetric in form and equal in amplitude, while the center element (measuring the vertical strain) measures minimal strain. The strain measurements for the +Y side do not represent any expected response. The time history response for each strain element is different in both shape and amplitude. All indications were that there was an error with the strain measurements, consequently discarded.

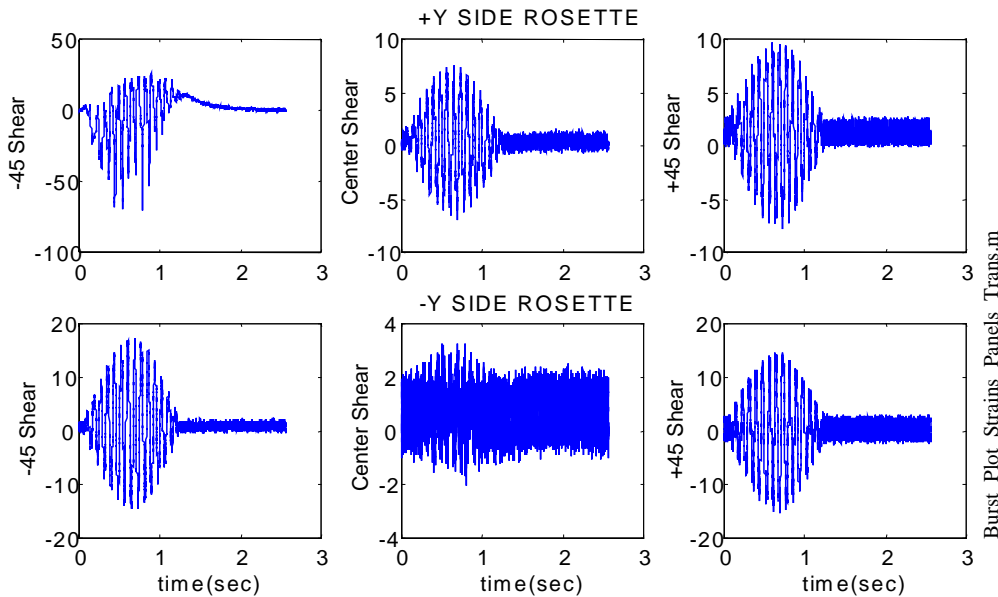


Figure 11-8. Strain gage data recorded for the $\pm Y$ side shear panels. The $\pm 45^\circ$ strain elements and vertical strain element are shown and compared for both shear panels. Measurement values are given in units of Micro-Strains.

The in-plane stresses in the -Y side shear panel were calculated from the strain measurements. The principal stresses and maximum shear stress are shown in Figure 11-9. The maximum principal stress was computed to be 2540 psi and the minimum principal stress was computed to be -2073 psi. The maximum shear stress at any point in-plane of the shear panel is 1270 psi.

The computed stress values were compared to the yield stress of the parent material, 6061-T6 aluminum. 6061-T6 aluminum has a yield stress of 37 ksi in tension and 20 ksi in shear, resulting in a factor of safety of 14 for tension and 15.7 for shear. One must also note, however, that the stress levels of the calorimeter are dependent on the

stiffness of the test fixture (recall the fixture stiffness is ~600 Hz) or the structure supporting the calorimeter. Recall, the calorimeter is constrained at the top through attachment locations in four places to the test fixture. The test fixture stiffness will therefore restrict the lateral deformations of the calorimeter, thus reducing the stress from that of the unconstrained boundary condition. The reported stresses can be corrected by properly scaling them, once the grid stiffness and boundary conditions are known.

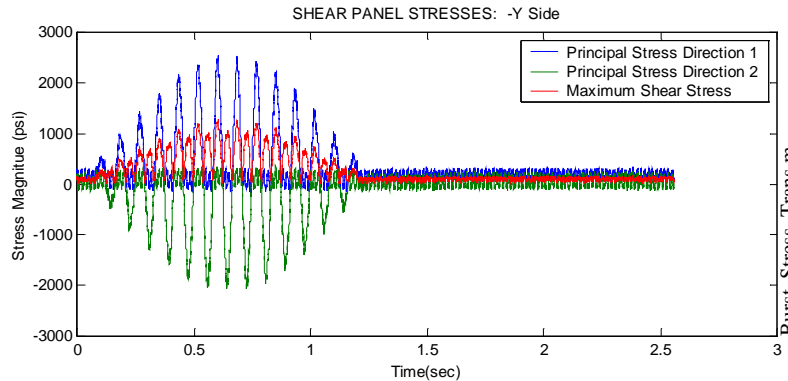


Figure 11-9. Plot showing the principal stresses and maximum shear stresses computed for the calorimeter shear panels.

11.2 Thrust Axis Test Results

11.2.1 Random Vibration Test

The Shake Test 99 calorimeter was subjected to three levels of random vibration in the thrust (vertical) direction as described in Section 6 & 8. During the tests, the experimental transfer functions were recorded using an FFT analyzer. The results from the thrust axis tests are described herein.

The primary goal of the thrust axis test was to identify the fundamental vertical mode of the calorimeter. The CsI stack is less susceptible to damage due to motions in the vertical direction, however the knowledge gained from the vibration tests can be used in analytical models to predict the response of the structure when subjected to the launch environment. The vertical transfer function is shown in Figure 11-10 for seven of the measurement locations on the calorimeter relative to the base. The seven locations include four of the CsI logs on different rows, two on the shear panels and one on the top compression panel.

Examination of the transfer functions reveal that the fundamental mode is ~200 Hz and the damping ratio is lower than that of the 1st transverse mode (indicated by the narrow bandwidth of the peak). The test fixture fundamental mode is just higher than 500 Hz. The test fixture peak at ~200 Hz is believed to be a result of the coupled response of the calorimeter and test fixture top plate. The mode shape is believed to be an oil canning response of the top plate that was created by the vertical accordion motion of the calorimeter. The higher amplitude of the CsI logs and calorimeter top panel with respect to the test fixture provide an indication that the fundamental mode at 200 Hz is a calorimeter mode and not a test fixture mode.

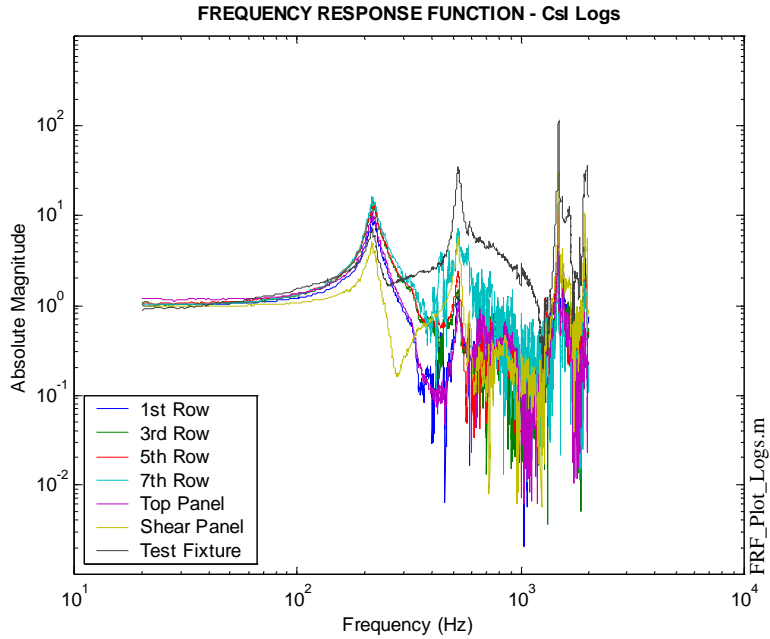


Figure 11-10. Plot of the vertical transfer function from the base to the measurement location. Transfer functions for four of the eight CsI logs, the top compression panel, shear panel and test fixture are shown.

Further analysis was performed to determine the natural frequencies, mode shapes, damping ratios and quality factors of the calorimeter using the modal identification software package^[9]. Seven measurement locations were used in the modal analysis including four from the CsI logs, two from the shear panels and one from the top compression plate. The test fixture response was not considered. The experimental transfer function is plotted together with the best-fit transfer function in Figure 11-11. Only one response location used in the analysis is shown here (all of the response locations used for the modal analysis are shown in Appendix D).

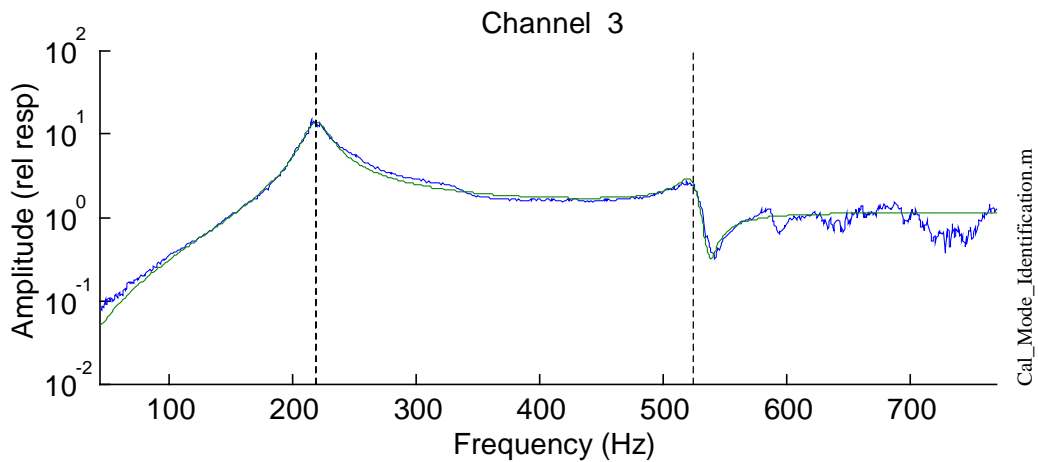


Figure 11-11. Plot of the experimental vertical transfer function (blue) and the numerically estimated vertical transfer function (green) used in the modal identification analysis.

The modal identification routine was able to identify two of the modes with a high degree of confidence. The damping ratios were also identified with a high degree of confidence, unlike the higher modes of the transverse direction test. The natural frequencies (f), damping ratios (ζ) and quality factors (Q) are given in Table 11-2 and are compared to the simulation results from the MATLAB model (lumped mass).

Table 11-2. Dynamic properties identified from the experimental results and compared to the MATLAB model simulations.

Mode	MATLAB	Experimental		
	Frequency	Frequency	Damping Ratio	Quality Factor
1 st Vertical (Accordion)	305.4 Hz	218.5 Hz	4.1%	12.2
2 nd Vertical (Accordion)	598.9 Hz	524 Hz	1.4%	35.7

The natural frequencies predicted by the MATLAB simulations are notably different from the experimental results. This is a direct result of the fixed boundary conditions used in the MATLAB model. The analytical model uses rigid boundary conditions to constrain the top compression panel at four points. The experimental boundary conditions imitate these constraints, although the less-than-rigid test fixture is substituted for the rigid MATLAB supports. The end result is a coupling of the test fixture and calorimeter stiffness, thus reducing the natural frequencies extracted from the experimental results.

In addition to the dynamic properties, the modal identification analysis was able to identify the two mode shapes associated with the two frequency poles. The two experimental mode shapes are shown in Figure 11-12 and compared to the undeformed shape. The fundamental mode is an accordion mode of the CsI stack that is characterized by the motion of all four layers of logs moving vertically in-phase, as shown in the middle figure. The second mode is also an accordion mode, but is more difficult to distinguish from the model below. From the mode shape data, it is known that as the top CsI log and top compression panel are moving in the positive vertical direction, the bottom three CsI logs are moving 180° out-of-phase, in the negative direction.

The agreement between experimental and MATLAB mode shapes is excellent. The predicted MATLAB mode shapes are shown in Figure 11-13 and compared to the undeformed shape. Here, the first transverse mode is clearly an accordion mode of the CsI stack. All eight layers of logs are moving vertically in-phase, as with the experimental mode in Figure 11-12. The second mode is more identifiable with the analytical model. The mode shape is the second accordion mode of the CsI stack. The upper half of the CsI stack is moving in the positive vertical direction, while the lower half is moving 180° out-of-phase, in the negative vertical direction.

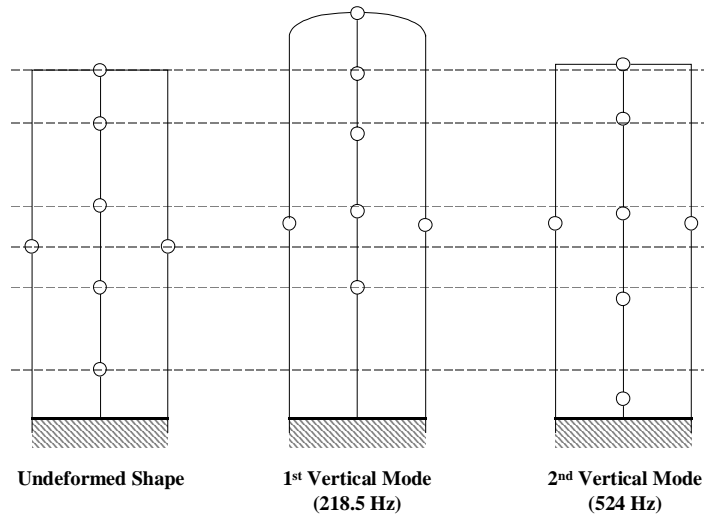


Figure 11-12. Illustration of the first two vertical CsI stack modes extracted from the experimental results. The undeformed shape is shown for reference.

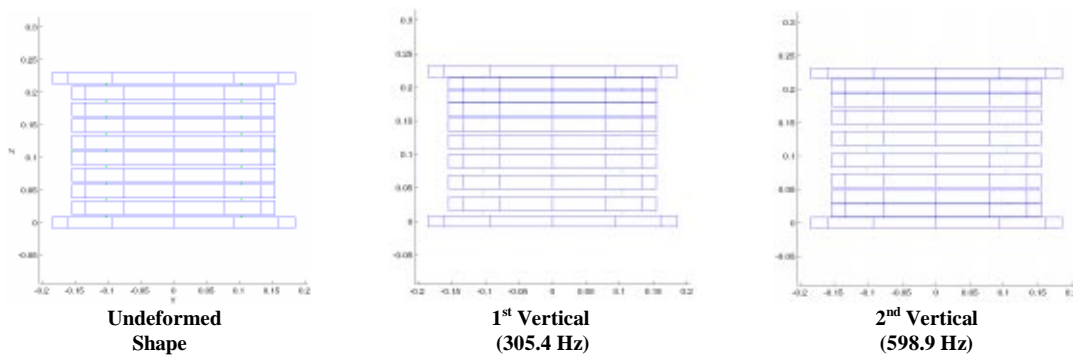


Figure 11-13. Illustration of the first two vertical CsI stack modes as predicted by MATLAB. The undeformed shape is shown for reference.

As with the transverse tests, the response of the CsI stack was shown to be amplitude dependent. The fundamental frequency increased by ~ 9.8% to ~240 Hz and the damping ratio decreased when the dynamic amplitude was decreased to 0.15 g's for the low-level random vibration tests. This is illustrated in Figure 11-14.

Again, the amplitude dependence, both frequency shift and order of magnitude, of the CsI stack was expected. Typical rubber compounds are known to exhibit nonlinear stiffness characteristics demonstrated in these tests. Similar characteristics were also observed in an earlier random vibration test performed on three CsI logs sandwiched between two layers of a similar rubber compound. Further discussions about the behavior of rubber compounds can be reviewed in Section 11.1.1.

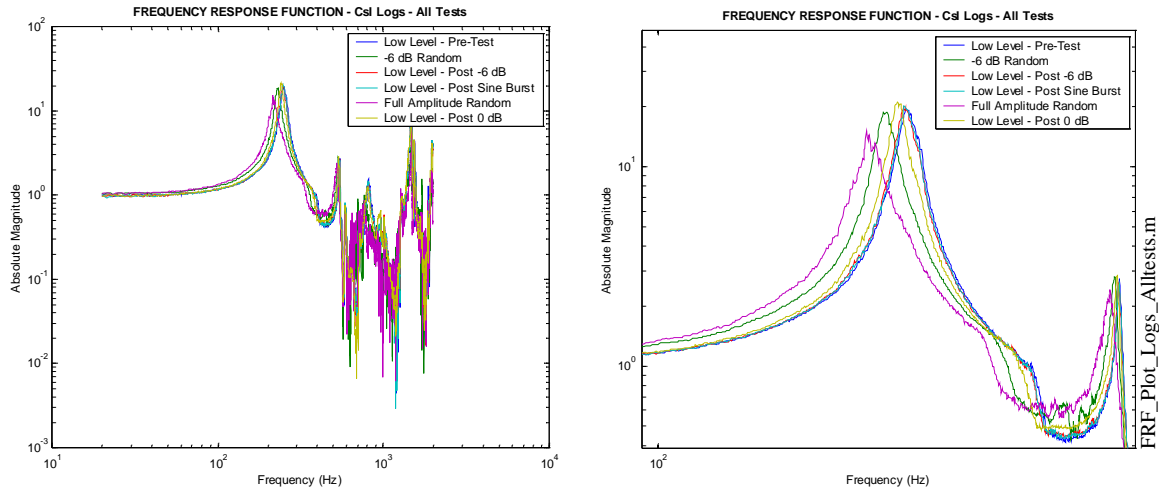


Figure 11-14. Plot of the vertical transfer function for all six random vibration tests (left). The transfer function is from the base to the CsI log located at the center of the calorimeter. A blowup of the fundamental peak is shown for clarity (right).

11.2.2 Sine Burst Test

The sine burst test was also performed for the thrust axis to validate the design and workmanship to the limit load factors used in the design analyses. The sine burst test subjected the calorimeter to a quasi-static qualification level acceleration of 8.25 g's at 15 Hz. The time history acceleration and strain response was recorded for analysis.

As with the transverse axis tests, it is difficult to draw many conclusions from the acceleration time history data other than the design and workmanship has successfully withstood the qualification level sine burst test along the thrust axis. The calorimeter can be expected to survive the static equivalent launch environment without damage. Post-test inspection and a low-level random vibration characterization (before and after the sine burst test), confirm that there was no damage during testing. Figure 11-15 is a plot of the low-level random vibration characterization that was performed before all testing, after the 1/2 amplitude sine burst test and again after the full amplitude sine burst test. Figure 11-16 is shown to demonstrate that only the expected acceleration response was measured during the sine burst test.

Strain measurements were also recorded during the vertical sine burst test. One goal of taking the strain measurements was to measure the in-plane strain in the shear panels and compute the in-plane principal and shear stresses. Each of the four shear panels was instrumented with a single strain rosette. The response of the two Y side panels was recorded and the stresses were computed. Additional strain measurements were taken on the containment panels, however limited information about the stress-state was known and the in-plane stresses could not be accurately computed.

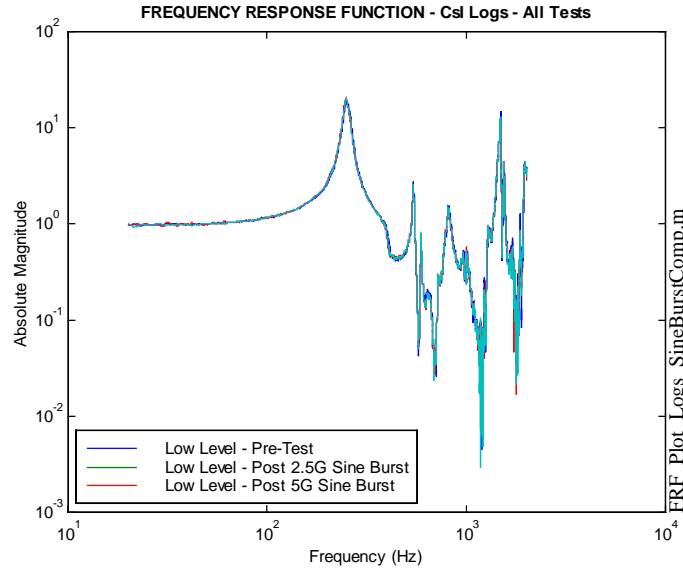


Figure 11-15. Plot of the vertical transfer function for the three low-level random vibration characterization tests performed before all tests, after the 1/2 amplitude sine burst test and again after the full amplitude sine burst test.

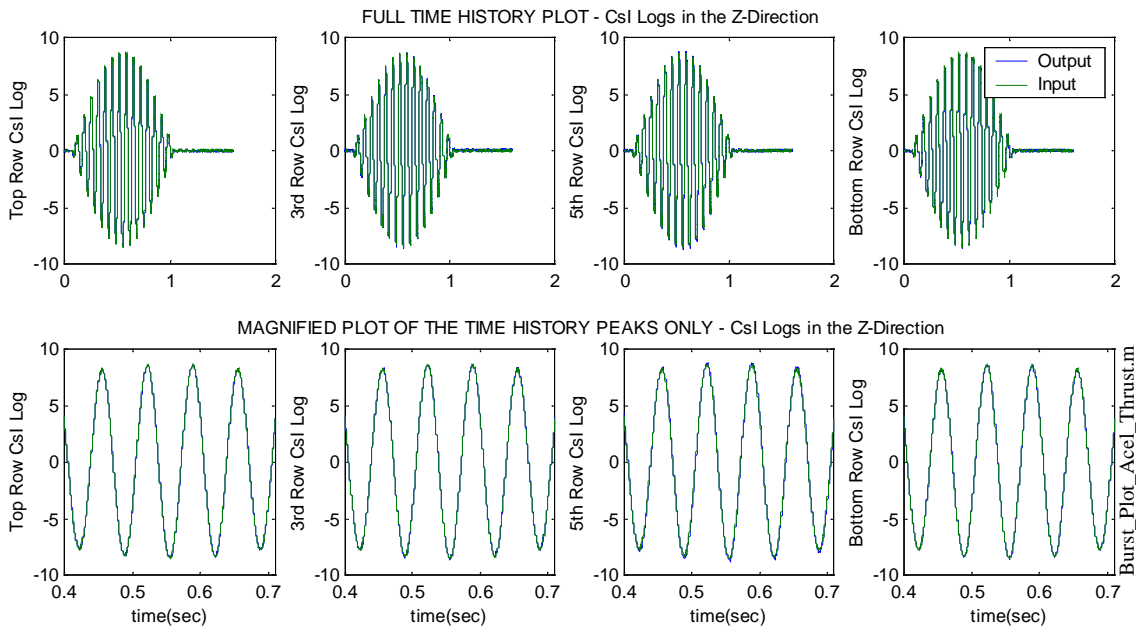


Figure 11-16. Time history response (blue), in g's, for the four Csl layers measured. Magnification of the time history is shown for clarity and the base acceleration (green) is shown for reference.

Figure 11-17 shows the shear panel strain measurements recorded during the full amplitude sine burst test (additional strain measurements are shown in Appendix E). The top three plots are the strain measurements for the +Y side and the bottom three plots are the strain measurements for the -Y side. The -Y side response illustrates the expected response of a panel subjected to axial deformations. All three elements are symmetric in form and equal in

amplitude. The strain measurements for the +Y side do not represent any expected response. The time history response for each strain element is different in both shape and amplitude. All indications are that there was an error with the strain measurements, consequently discarded.

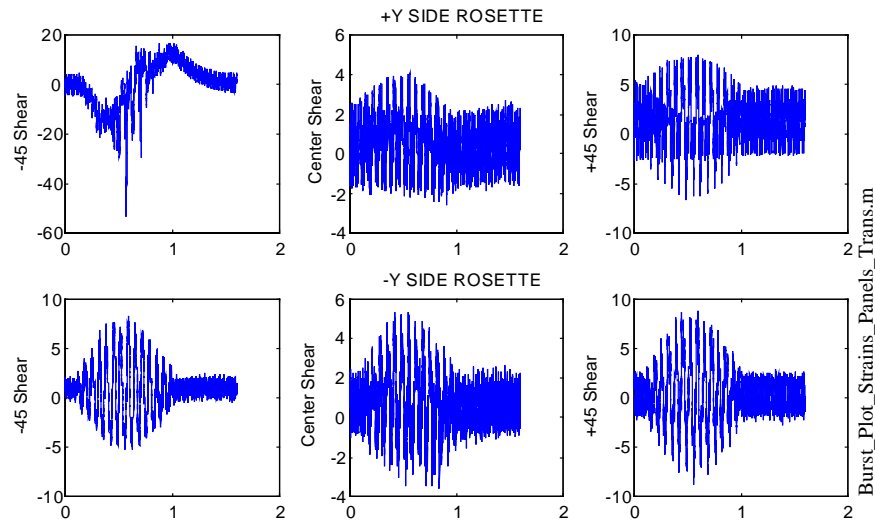


Figure 11-17. Strain gage data recorded for the $\pm Y$ side shear panels. The $\pm 45^\circ$ strain elements and vertical strain element are shown and compared for both shear panels. Measurement values are given in units of Micro-Strains.

The in-plane stresses in the -Y side shear panel were calculated from the strain measurements. The principal stresses and maximum shear stress are shown in Figure 11-18. The maximum principal stress was computed to be 1189 psi and the minimum principal stress was computed to be -921 psi. The maximum shear stress at any point in-plane of the shear panel is 824 psi.

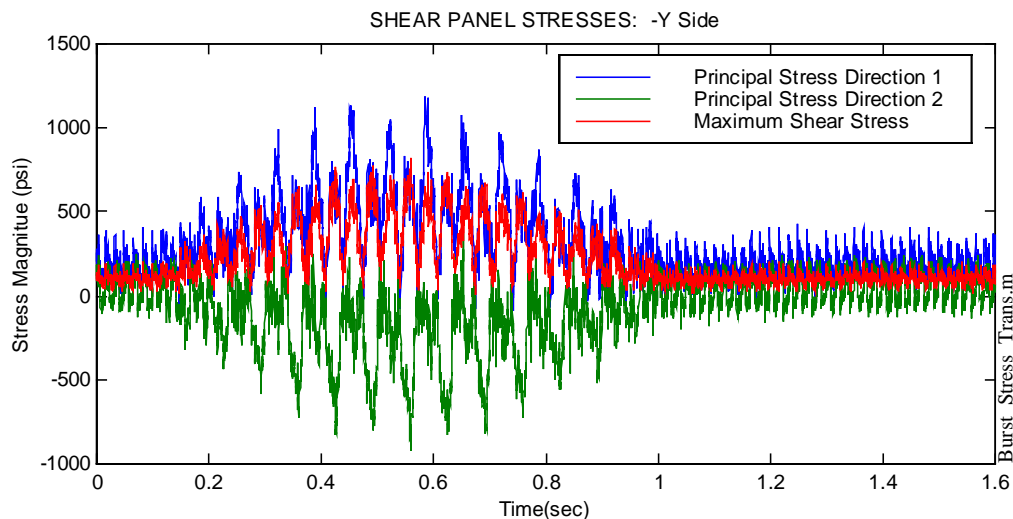


Figure 11-18. Plot showing the principal stresses and maximum shear stresses computed for the calorimeter shear panels.

The computed stress values were compared to the yield stress of the parent material, 6061-T6 aluminum. 6061-T6 aluminum has a yield stress of 37 ksi in tension and 20 ksi in shear, resulting in a factor of safety of 31 for tension and 24 for shear. One must also note, however, that the stress levels of the calorimeter are dependent on the stiffness of the test fixture (recall the fixture stiffness is ~500 Hz) or the structure supporting the calorimeter. Recall, the calorimeter is constrained at the top through attachment locations in four places to the test fixture. The test fixture stiffness will therefore restrict the vertical deformations of the calorimeter, thus reducing the stress from that of the unconstrained boundary condition. The reported stresses can be corrected by properly scaling them, once the grid stiffness and boundary conditions are known.

12. References

1. *General Environmental Specification for STS & ELV Payloads, Subsystems, and Components*, GEVS-SE Rev. A, System Reliability and Safety Office, Code 302, NASA/Goddard Space Flight Center, Greenbelt, MD, June 1996.
2. E. Ponslet, F. Biehl, W. O. Miller, and R. Smith, "Conceptual Mechanical Design of a CsI Calorimeter for GLAST," HYTEC Inc., HYTEC-TN-GLAST-03, June 1998.
3. F. Biehl, and E. Ponslet, "GLAST Calorimeter Static and Dynamic Structural Response to Launch Environment," HYTEC Inc., HYTEC-TN-GLAST-01, June 1998.
4. E. Swensen and E. Ponslet, "GLAST Shake Test 99 Calorimeter Random Vibration Test Plan," HYTEC Inc., HYTEC-TN-GLAST-09, September 1999.
5. *Shock and Vibration Handbook*, 4th edition, C. M. Harris, editor, McGraw-Hill, 1996.
6. *GLAST Science Instruments – Spacecraft Interface Requirements Document*, August 3, 1999.
7. *NRL Naval Center for Space Technology, Process Specification, Installation of Bolts, Screws, Washers, Nuts and Hi-Lok Fasteners*, SSD-PS-018M Rev M, March 1, 1999.
8. Matlab Software, The MathWorks, Inc., 24 Prime Park Way, Natick, MA 017060, <http://www.mathworks.com>.
9. *Structural Dynamics Toolbox* for Matlab, E. Balmes, Ed., Scientific Software Group, <http://www.ssg.fr/sdt>, 20 rue Troyon, 92136 Sevres, France, 1997.

13. Appendix A: Test Summary – As Performed

The following table lists the tests performed on the Shake Test 99 Calorimeter. The order, times performed and control channel are also listed. The Transverse Axis tests were performed on September 23, 1999 and the Thrust Axis tests were performed on September 24, 1999. HYTEC personnel were not present during the Thrust axis tests, therefore time information is not available.

13.1 Test Summary for the Transverse Axis

Shake Test 99 Calorimeter Test Summary – Transverse Axis					
Run	Time	Test Description	Axis	Control	File Name
		Transverse Shaker Operation Evaluation Test			
		Wedge Check 5 gpk at 20 Hz (0.25" pk-pk)	X		
		Random 6.81 grms 20-2000 Hz: 60 sec : Pre-Test	X		
		Sine Burst 5 gpk at 10 Hz : 5 cycles : Pre-Test	X		
		Calorimeter Test Parallel to the Transverse Axis			
1	12:28	Instrumentation Check 0.25 gpk at 20 Hz	X	121	
1	12:36	Sine Sweep 0.5 gpk 10-2000 Hz : 4 Oct/min	X	121	RUN1
2	15:00	Low Level Random 0.45 grms, 10-2000 Hz	X	Max(121,122)	RUN2
3	15:45	Sine Burst 2.5 gpk at 10 Hz : 5 cycles (approximate)	X	Max(121,122)	RUN3
		Sine Sweep 0.5 gpk 10-2000 Hz : 4 Oct/min			
4	16:18	Random -6dB x 6.81 grms 20-2000 Hz : 60 sec	X	Max(121,122)	RUN4
		Sine Sweep 0.5 gpk 10-2000 Hz : 4 Oct/min	X		
5	16:45	Low Level Random 0.45 grms, 10-2000 Hz	X	Max(121,122)	RUN5
6	17:10	Sine Burst 5 gpk at 12 Hz : 5 cycles	X	Max(121,122)	RUN6
		Sine Sweep 0.5 gpk 10-2000 Hz : 4 Oct/min	X		
7	17:22	Low Level Random 0.45 grms, 10-2000 Hz	X	Max(121,122)	RUN7
		Random 6.81 grms 20-2000 Hz : 60 sec : Limited	X		
		Sine Sweep 0.5 gpk 10-2000 Hz : 4 Oct/min	X		
8	17:40	Random 6.81 grms 20-2000 Hz : 60 sec : No Limit	X	Max(121,122)	RUN8
		Sine Sweep 0.5 gpk 10-2000 Hz : 4 Oct/min			
9	17:52	Low Level Random 0.45 grms, 10-2000 Hz	X	Max(121,122)	RUN9
		Random 6.81 grms 20-2000 Hz : 60 sec : No Limit (with PC Board included in calorimeter assembly)	X		
		Sine Sweep 0.5 gpk 10-2000 Hz : 4 Oct/min	X		

13.2 Test Summary for the Thrust Axis

Shake Test 99 Calorimeter Test Summary – Thrust Axis					
Run	Time	Test Description	Axis	Control	File Name
		Thrust Shaker Operation Evaluation Test			
		Wedge Check 5 gpk at 20 Hz (0.25" K-F)	Z		
		Random 6.81 grms 20-2000 Hz: 60 sec : Pre-Test	Z		
		Sine Burst 8.25 gpk at 12.7 Hz : 5 cycles : Pre-Test	Z		
		Calorimeter Test Parallel to the Thrust Axis			
10	?	Instrumentation Check 0.25 gpk at 20 Hz	Z	121	
		Sine Sweep 0.5 gpk 10-2000 Hz : 1 Oct/min	Z		
10	?	Low Level Random 0.45 grms, 10-2000 Hz	Z	Max(121,122)	RUN10
11	?	Sine Burst 4.125 gpk at 15 Hz : 5 cycles	Z		RUN11
		Sine Sweep 0.5 gpk 10-2000 Hz : 1 Oct/min	Z		
12	?	Random -6dB x 6.81 grms 20-2000 Hz : 30 sec	Z		RUN12
		Sine Sweep 0.5 gpk 10-2000 Hz : 1 Oct/min	Z		
13	?	Low Level Random 0.45 grms, 10-2000 Hz	Z	Max(121,122)	RUN13
14	?	Sine Burst 8.25 gpk at 15 Hz : 5 cycles	Z		RUN14
		Sine Sweep 0.5 gpk 10-2000 Hz : 1 Oct/min	Z		
15	?	Low Level Random 0.45 grms, 10-2000 Hz	Z	Max(121,122)	RUN15
		Random 6.81 grms 20-2000 Hz : 60 sec : Limited	Z		
		Sine Sweep 0.5 gpk 10-2000 Hz : 4 Oct/min	Z		
16	?	Random 6.81 grms 20-2000 Hz : 60 sec : No Limit	Z		RUN16
		Sine Sweep 0.5 gpk 10-2000 Hz : 1 Oct/min	Z		
17	?	Low Level Random 0.45 grms, 10-2000 Hz	Z	Max(121,122)	RUN17

14. Appendix B: Accelerometer Locations

The following are tables to record accelerometer locations for the random vibration tests performed on the Shake Test 99 Calorimeter.

14.1 Vibration Testing Parallel to the Transverse Axis

Accelerometer Information for the Transverse Axis Tests							
Location No.	Cable No.	Channel No.	Type	Serial No.	Sensitivity (pC/g)	Test Axis	Location
Shaker Table Instrumentation (Input Control Channel)							
1	•	•	•	•	•	•	Shaker Table Near Test Fixture
Calorimeter Instrumentation							
2	1	3	2222C	13703	1.327	+X	CsI Replacement Logs, +X Side, 1 st Row Left
3	2	4	2222C	13774	1.302	+X	CsI Replacement Logs, +X Side, 1 st Row Right
4	3	5	2222C	13707	1.400	+X	CsI Replacement Logs, +X Side, 2 nd Row Left
5	4	6	2222C	13839	1.294	+X	CsI Replacement Logs, +X Side, 2 nd Row Right
6	5	7	2222C	13671	1.298	+X	CsI Replacement Logs, +X Side, 3 rd Row Left
7	6	8	2222C	13640	1.371	+X	CsI Replacement Logs, +X Side, 3 rd Row Right
8	7	9	2222C	13794	1.488	+X	CsI Replacement Logs, +X Side, 4 th Row Left
9	8	10	2222C	13725	1.251	+X	CsI Replacement Logs, +X Side, 4 th Row Right
10	9	11	2222C	13693	1.207	+Y	CsI Replacement Logs, +Y Side, 1 st Row Left
11	10	12	2222C	13741	1.305	+X	CsI Replacement Logs, +Y Side, 1 st Row Right
12	11	13	2222C	13833	1.217	+X	CsI Replacement Logs, +Y Side, 2 nd Row Left
13	12	14	2222C	13630	1.241	+Y	CsI Replacement Logs, +Y Side, 2 nd Row Right
14	13	15	2222C	13684	1.374	+Z	Top Compression Panel, +X edge, Center
15	•	•	•	•	•	•	Top Compression Panel, +Y edge, Center
16	14	16	2222C	13762	1.306	+X	Shear Panel, +X Side, Top-Center
17	15	17	2222C	13777	1.355	+X	Shear Panel, +X Side, Center-Center
18	16	18	2222C	13783	1.326	+X	Shear Panel, +X Side, Bottom-Center
19.1	17	19	2222C	AC24	1.750	+X	Shear Panel, +Y Side, Center
19.2	18	20	2222C	AC61	1.497	+Y	Shear Panel, +Y Side, Center
19.3	19	21	2222C	AC80	1.711	+Z	Shear Panel, +Y Side, Center

20	20	22	2222C	13747	1.254	-X	Shear Panel, -X Side, Center
21.1	21	23	2222C	13737	1.384	-X	Shear Panel, -Y Side, Center
21.2	22	24	2222C	13760	1.309	-Y	Shear Panel, -Y Side, Center
21.3	23	25	2222C	13667	1.325	+Z	Shear Panel, -Y Side, Center
22	26	28	•	•	•	•	PC Board
23	27	29	•	•	•	•	PC Board
24	28	30	•	•	•	•	PC Board
Fixture Instrumentation							
25	29	31	2229C	CC22	3.077	+X	Long Shear Plate, +X Side, Top Center
26	30	32	2226C	FL31	2.56	+X	Long Shear Plate, +X Side, Center
27	121	1	7702-50	CA24	54.2	+X	Long Shear Plate, +X Side, Bottom Center
28	•	•	•	•	•	•	Shear Plate, +Y Side, Center
29	31	33	2226C	FL51	2.42	+Z	Top Plate, Center
30	32	34	2229C	CC33	2.844	+X	Long Shear Plate, +X Side, Top Left
31	•	•	•	•	•	•	Long Shear Plate, +X Side, Top Right
32	122	2	7702-50	CA23	52.6	+X	Long Shear Plate, +X Side, Bottom Left
33	•	•	•	•	•	•	Long Shear Plate, +X Side, Bottom Right
34	•	•	•	•	•	•	Shear Plate, +Y Side, Top Left
35	33	35	2229C	CC16	3.160	+Y	Shear Plate, +Y Side, Top Center
36	•	•	•	•	•	•	Shear Plate, +Y Side, Top Right
37	•	•	•	•	•	•	Shear Plate, +Y Side, Bottom Left
38	34	36	2229C	CC53	2.693	+Y	Shear Plate, +Y Side, Bottom Center
39	•	•	•	•	•	•	Shear Plate, +Y Side, Bottom Right
Additional Instrumentation							
40	24	26	2222C	BM03	1.779	+X	Containment Panel, +X Side, Left Center
41	25	27	2222C	BA84	1.778	+X	Containment Panel, +X Side, Right Center
42							
43							

14.2 Vibration Testing Parallel to the Thrust Axis

Accelerometer Information for the Thrust Axis Tests							
Location No.	Cable No.	Channel No.	Type	Serial No.	Sensitivity (pC/g)	Test Axis	Location
Shaker Table Instrumentation (Input Control Channel)							
1.1	121	1	7702-50	CA24	54.2	+Z	Shaker Table Near Test Fixture
1.2	122	2	7702-50	CA23	52.6	+Z	Shaker Table Near Test Fixture
Calorimeter Instrumentation							
2	1	3	2222C	13703	1.327	+Z	CsI Replacement Logs, +X Side, 1 st Row Left
3	2	4	2222C	13774	1.302	+Z	CsI Replacement Logs, +X Side, 1 st Row Right
4	3	5	2222C	13707	1.400	+Z	CsI Replacement Logs, +X Side, 2 nd Row Left
5	4	6	2222C	13839	1.294	+Z	CsI Replacement Logs, +X Side, 2 nd Row Right
6	5	7	2222C	13671	1.298	+Z	CsI Replacement Logs, +X Side, 3 rd Row Left
7	6	8	2222C	13640	1.371	+Z	CsI Replacement Logs, +X Side, 3 rd Row Right
8	7	9	2222C	13794	1.488	+Z	CsI Replacement Logs, +X Side, 4 th Row Left
9	8	10	2222C	13725	1.251	+Z	CsI Replacement Logs, +X Side, 4 th Row Right
10	9	11	2222C	13693	1.207	+Y	CsI Replacement Logs, +Y Side, 1 st Row Left
11	10	12	2222C	13741	1.305	+X	CsI Replacement Logs, +Y Side, 1 st Row Right
12	11	13	2222C	13833	1.217	+X	CsI Replacement Logs, +Y Side, 2 nd Row Left
13	12	14	2222C	13630	1.241	+Y	CsI Replacement Logs, +Y Side, 2 nd Row Right
14	13	15	2222C	13684	1.374	+Z	Top Compression Panel, +X edge, Center
15	•	•	•	•	•	•	Top Compression Panel, +Y edge, Center
16	14	16	2222C	13762	1.306	+X	Shear Panel, +X Side, 1 st Row Center
17	15	17	2222C	13777	1.355	+X	Shear Panel, +X Side, 2 nd Row Center
18	16	18	2222C	13783	1.326	+X	Shear Panel, +X Side, 3 rd Row Center
19.1	17	19	2222C	AC24	1.750	+X	Shear Panel, +Y Side, Center
19.2	18	20	2222C	AC61	1.497	+Y	Shear Panel, +Y Side, Center
19.3	19	21	2222C	AC80	1.711	+Z	Shear Panel, +Y Side, Center
20	20	22	2222C	13747	1.254	-X	Shear Panel, -X Side, Center
21.1	21	23	2222C	13737	1.384	-X	Shear Panel, -Y Side, Center
21.2	22	24	2222C	13760	1.309	-Y	Shear Panel, -Y Side, Center

21.3	23	25	2222C	13667	1.325	+Z	Shear Panel, -Y Side, Center
22	26	28	•	•	•	•	None
23	27	29	•	•	•	•	None
24	28	30	•	•	•	•	None
Fixture Instrumentation							
25	29	31	2229C	CC22	3.077	+X	Long Shear Plate, +X Side, Top Center
26	30	32	2226C	FL31	2.56	+X	Long Shear Plate, +X Side, Center
27	•	•	•	•	•	•	Long Shear Plate, +X Side, Bottom Center
28	•	•	•	•	•	•	Shear Plate, +Y Side, Center
29	31	33	2226C	FL51	2.42	+Z	Top Plate, Center
30	32	34	2229C	CC33	2.844	+X	Long Shear Plate, +X Side, Top Left
31	•	•	•	•	•	•	Long Shear Plate, +X Side, Top Right
32	•	•	•	•	•	•	Long Shear Plate, +X Side, Bottom Left
33	•	•	•	•	•	•	Long Shear Plate, +X Side, Bottom Right
34	•	•	•	•	•	•	Shear Plate, +Y Side, Top Left
35	33	35	2229C	CC16	3.160	+Y	Shear Plate, +Y Side, Top Center
36	•	•	•	•	•	•	Shear Plate, +Y Side, Top Right
37	•	•	•	•	•	•	Shear Plate, +Y Side, Bottom Left
38	34	36	2229C	CC53	2.693	+Y	Shear Plate, +Y Side, Bottom Center
39	•	•	•	•	•	•	Shear Plate, +Y Side, Bottom Right
Additional Instrumentation							
40	24	26	2222C	BM03	1.779	+X	Containment Panel, +X Side, Left Center
41	25	27	2222C	BA84	1.778	+X	Containment Panel, +X Side, Right Center
42							
43							

15. Appendix C: Strain Gage Sensor Locations

The following table identifies the strain gage sensor locations for those mounted on the Shake Test 99 calorimeter.

Strain Gage Sensor Locations for All Tests										
No.	Type	Gage Factor	Location	Axis	Wire Pin-Out				Set-Up	
					Block No.	Red	White	Black	Calibration Value	Signal Conditioner
E1	CEA-13-250UW-120	2.090 ±0.5%	Containment Panel, +X Side, Left Edge	Z	•	•	•	•	•	•
E2	CEA-13-250UW-120	2.090 ±0.5%	Containment Panel, +X Side, Middle	Z	•	•	•	•	•	•
E3	CEA-13-250UW-120	2.090 ±0.5%	Containment Panel, +X Side, Right Edge	Z	1	1	2	3	3828	1
F1	CEA-13-250UW-120	2.090 ±0.5%	Containment Panel, +Y Side, Left Edge	Z	1	4	5	6	3828	2
F2	CEA-13-250UW-120	2.090 ±0.5%	Containment Panel, +Y Side, Middle	Z	1	7	8	9	3828	3
F3	CEA-13-250UW-120	2.090 ±0.5%	Containment Panel, +Y Side, Right Edge	Z	1	10	11	12	3828	4
G1	CEA-13-250UW-120	2.090 ±0.5%	Containment Panel, -X Side, Left Edge	Z	1	13	14	15	3828	5
G2	CEA-13-250UW-120	2.090 ±0.5%	Containment Panel, -X Side, Middle	Z	1	16	17	18	3828	6
G3	CEA-13-250UW-120	2.090 ±0.5%	Containment Panel, -X Side, Right Edge	Z	1	19	20	21	3828	7
H1	CEA-13-250UW-120	2.090 ±0.5%	Containment Panel, -Y Side, Left Edge	Z	2	1	2	3	3828	19
H2	CEA-13-250UW-120	2.090 ±0.5%	Containment Panel, -Y Side, Middle	Z	2	4	5	6	3828	20
H3	CEA-13-250UW-120	2.090 ±0.5%	Containment Panel, -Y Side, Right Edge	Z	2	7	8	9	3828	21
L1	CEA-13-250UW-120	2.090 ±0.5%	Top Compression Panel, Middle	X	1	22	23	24	3828	8
L2	CEA-13-250UW-120	2.090 ±0.5%	Top Compression Panel, Middle	Y	1	25	26	27	3828	9

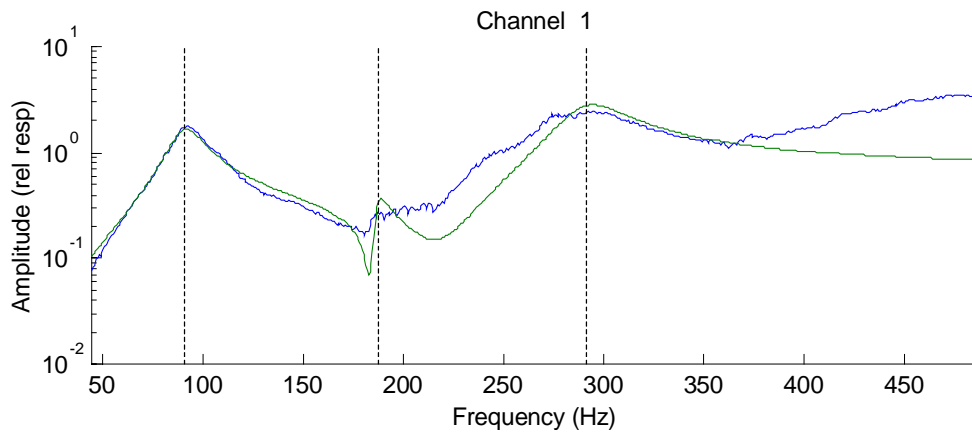
K1	CEA-13-250UW-120	2.090 ±0.5%	Bottom Compression Panel, Middle	X	1	28	29	30	3828	10
K2	CEA-13-250UW-120	2.090 ±0.5%	Bottom Compression Panel, Middle	Y	1	31	32	33	3828	11
•	CEA-13-125UR-120 (Rosette)	2.110 ±0.5%	Shear Panel, +X Side, Middle	-45°	•	•	•	•	•	•
•		2.145 ±0.5%		Z	•	•	•	•	•	•
•		2.110 ±0.5%		+45°	•	•	•	•	•	•
M1	CEA-13-125UR-120 (Rosette)	2.110 ±0.5%	Shear Panel, +Y Side, Middle	-45°	1	34	35	36	3791	12
M2		2.145 ±0.5%		Z	1	37	38	39	3730	13
M3		2.110 ±0.5%		+45°	1	40	41	42	3791	14
•	CEA-13-125UR-120 (Rosette)	2.110 ±0.5%	Shear Panel, -X Side, Middle	-45°	•	•	•	•	•	•
•		2.145 ±0.5%		Z	•	•	•	•	•	•
•		2.110 ±0.5%		+45°	•	•	•	•	•	•
N1	CEA-13-125UR-120 (Rosette)	2.110 ±0.5%	Shear Panel, -Y Side, Middle	-45°	2	10	11	12	3791	22
N2		2.145 ±0.5%		Z	2	13	14	15	3730	23
N3		2.110 ±0.5%		+45°	2	16	17	18	3791	24

16. Appendix D: Mode Identification Results for the Full Amplitude Random Vibration Test

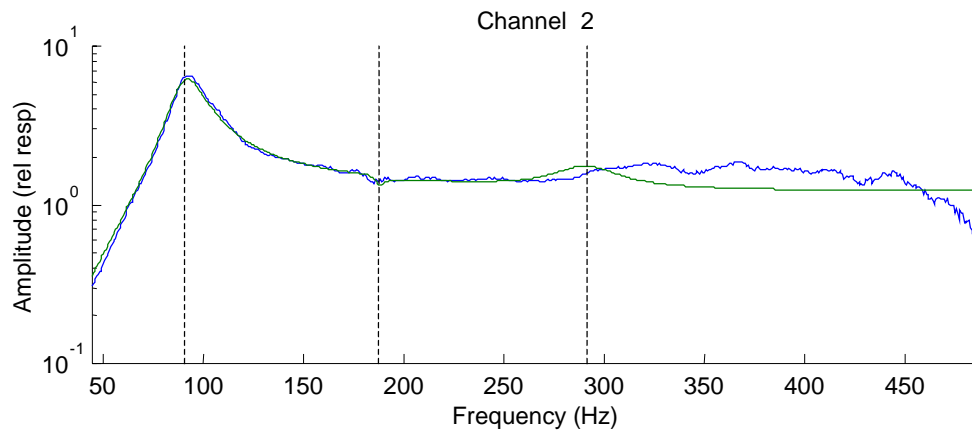
In this section, a collection of plots is shown that were used in the modal identification analysis. Each plot shows the experimental horizontal or vertical transfer function measured during the transverse and thrust axis tests, respectively. The numerical transfer function used to estimate the experimental transfer function is shown in green to illustrate the accuracy of the analysis.

16.1 Transverse Axis Results

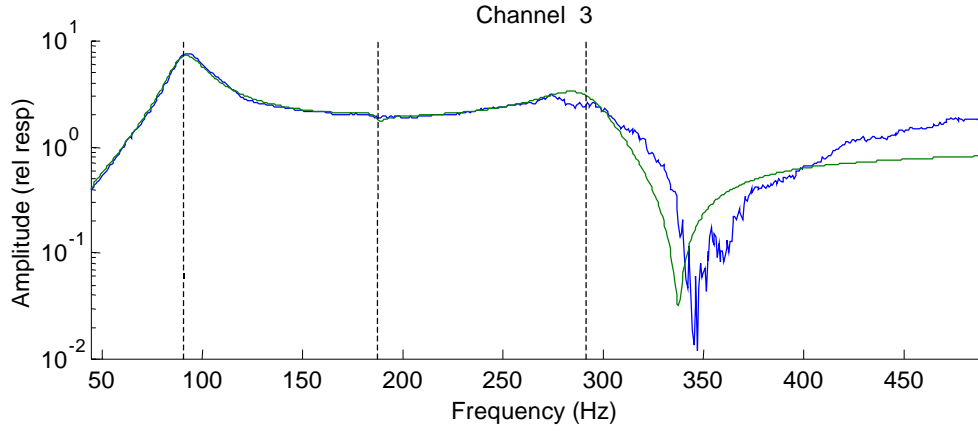
Using the modal identification software, three modes were identified. The natural frequencies are 91 Hz, 187 Hz and 292 Hz. The associated damping ratios are 9.3%, 1.9% and 6.05%, respectively. There is a high degree of confidence in the identified frequencies, however the only damping ratio that appears to be identified accurately is that of the fundamental mode.



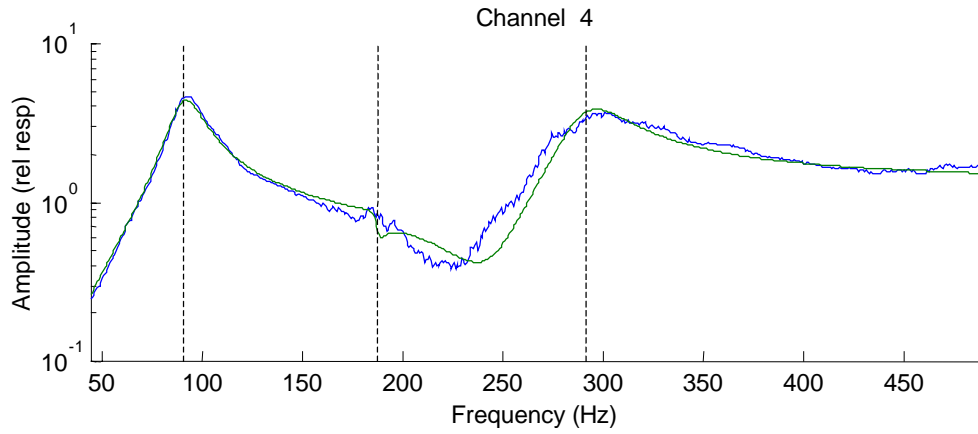
Response of the CsI Log on the top row (left), on the +X Side



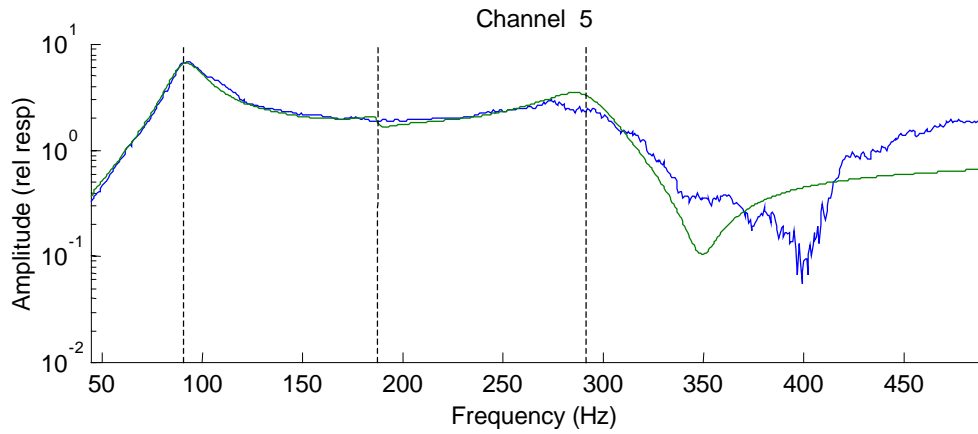
Response of the CsI Log on the 2nd row (left), on the +X Side



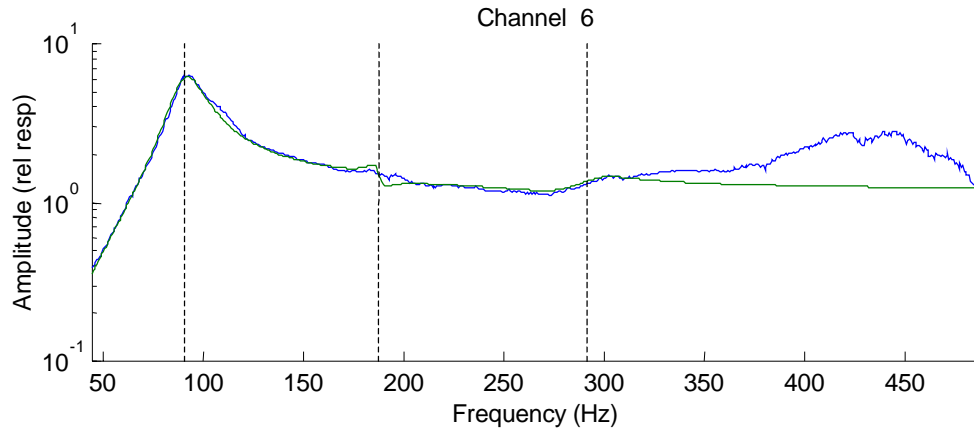
Response of the CsI Log on the 3rd row (left), on the +X Side



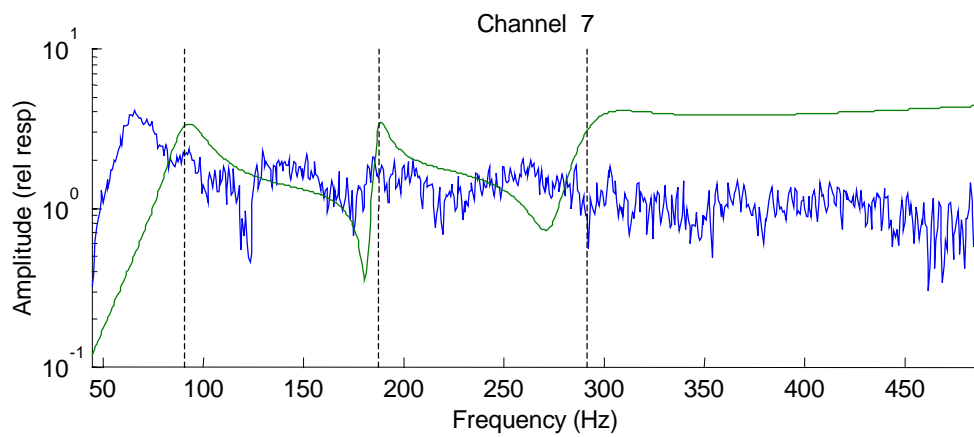
Response of the CsI Log on the bottom row (left), on the +X Side



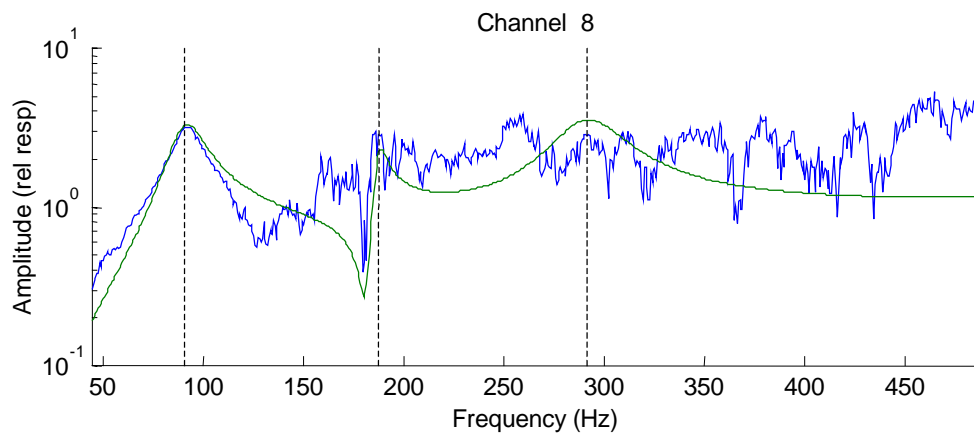
Response of the CsI Log on the top row (right), on the +Y Side



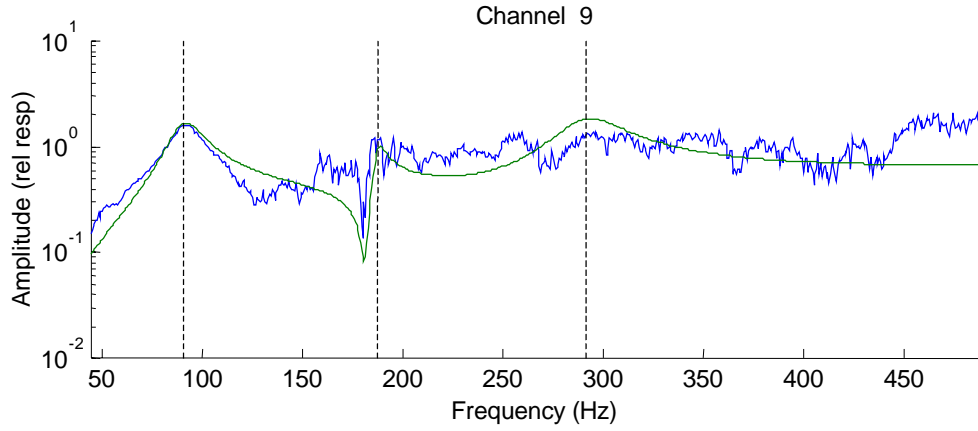
Response of the CsI Log on the bottom row (left), on the +Y Side



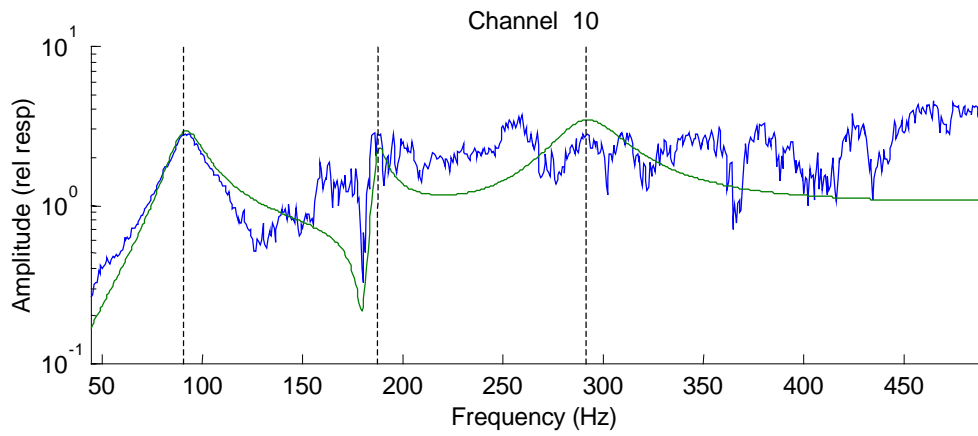
Response at the top of the shear panel, on the +X Side



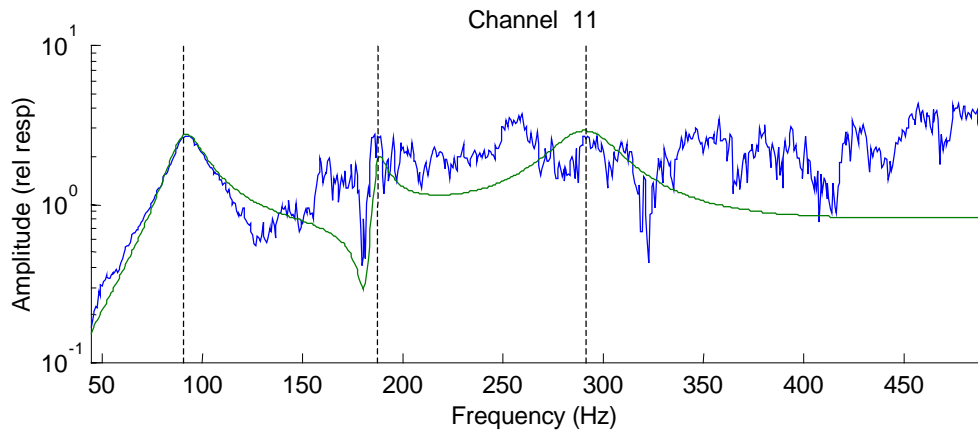
Response at the center of the shear panel, on the +X Side



Response at the bottom of the shear panel, on the +X Side



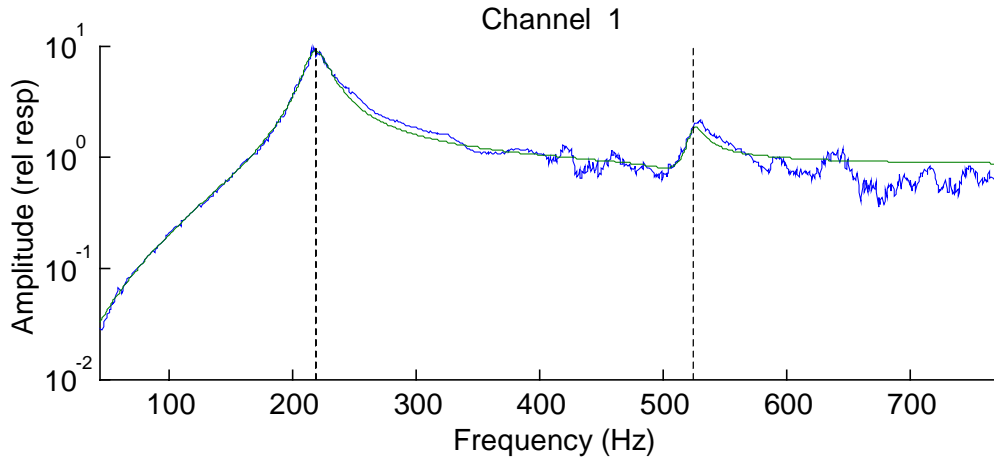
Response at the left of center of the containment panel, on the +X Side



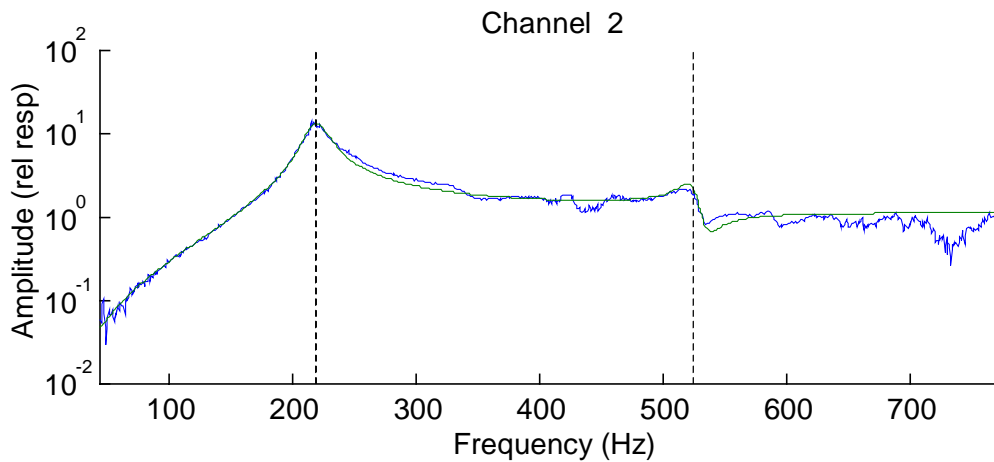
Response at the right of center of the containment panel, on the +X Side

16.2 Thrust Axis Results

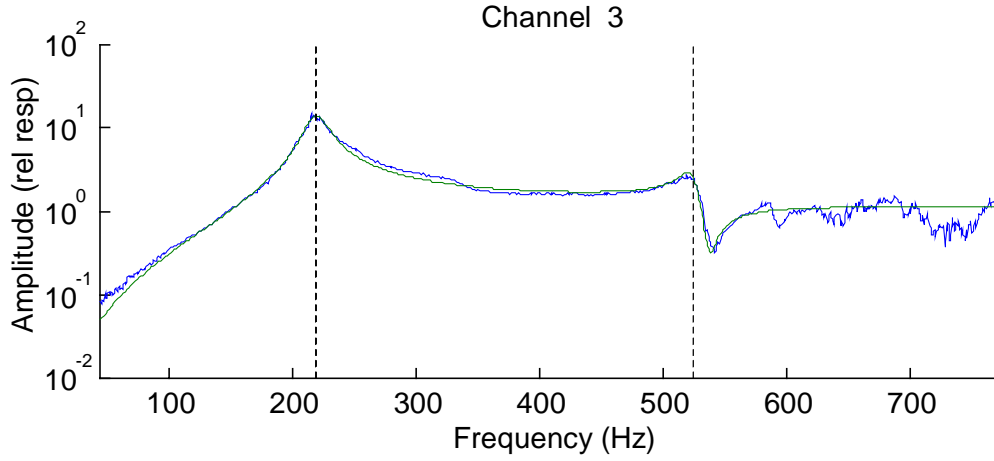
Using the modal identification software, two modes were identified. The natural frequencies are 218.5 Hz and 524 Hz. The associated damping ratios are 4.1% and 1.4%, respectively. There is a high degree of confidence in both the identified frequencies and damping ratios.



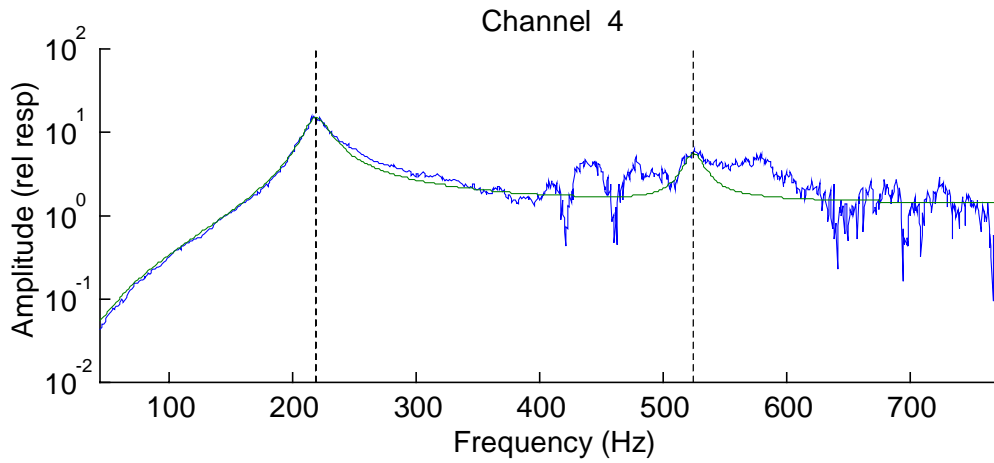
Response of the CsI Log on the top row (left), on the +X Side



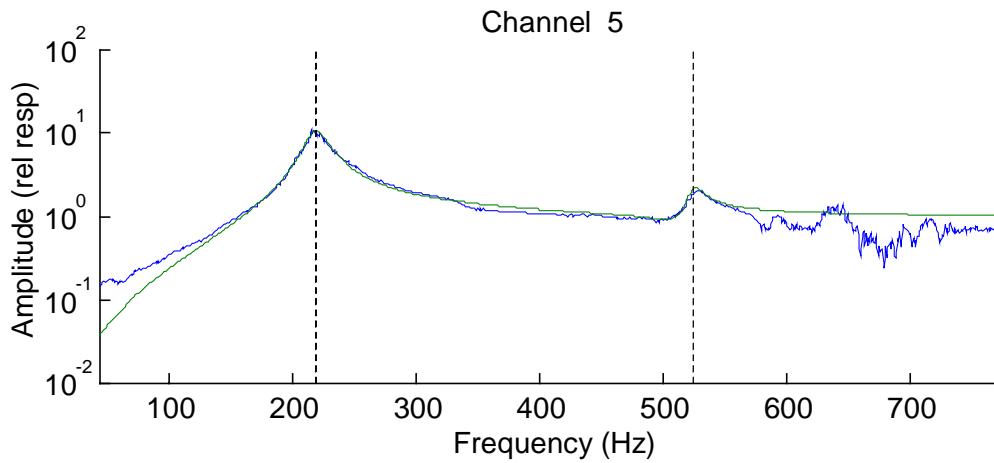
Response of the CsI Log on the 2nd row (left), on the +X Side



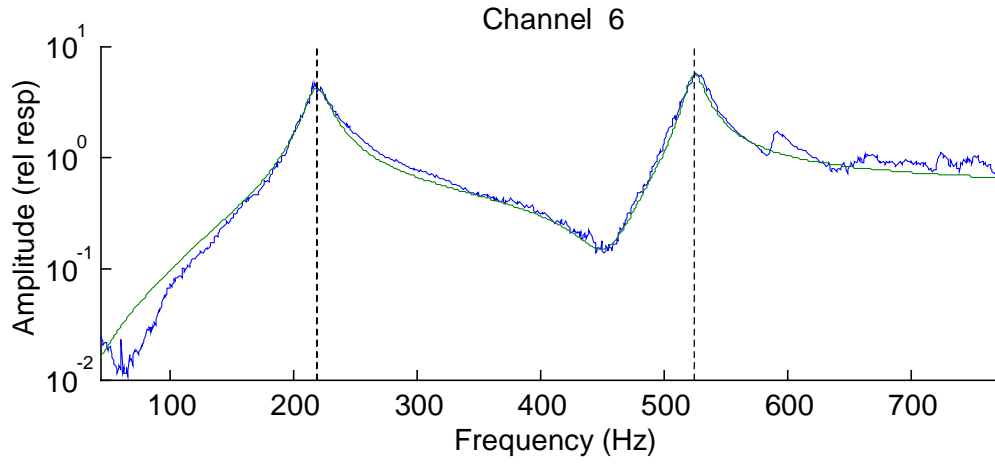
Response of the CsI Log on the 3rd row (left), on the +X Side



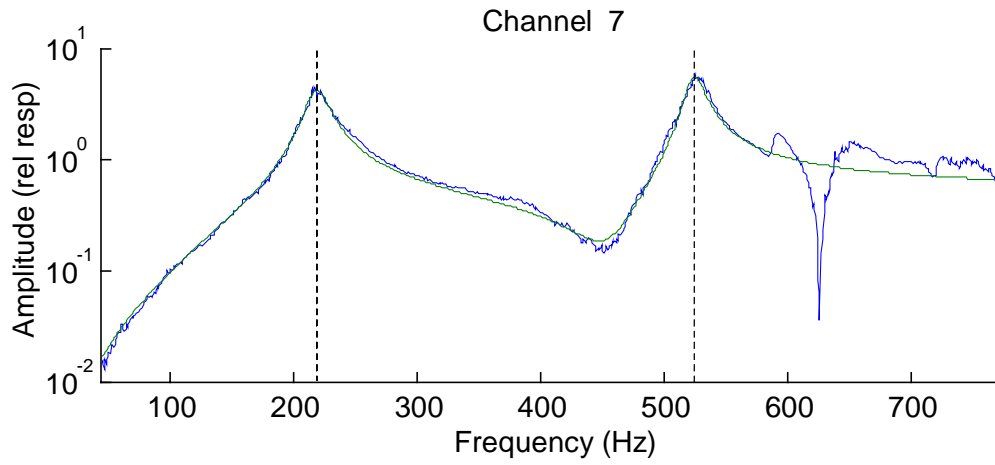
Response of the CsI Log on the bottom row (left), on the +X Side



Response at the center of the shear panel, on the +Y Side



Response at the center of the shear panel, on the -Y Side

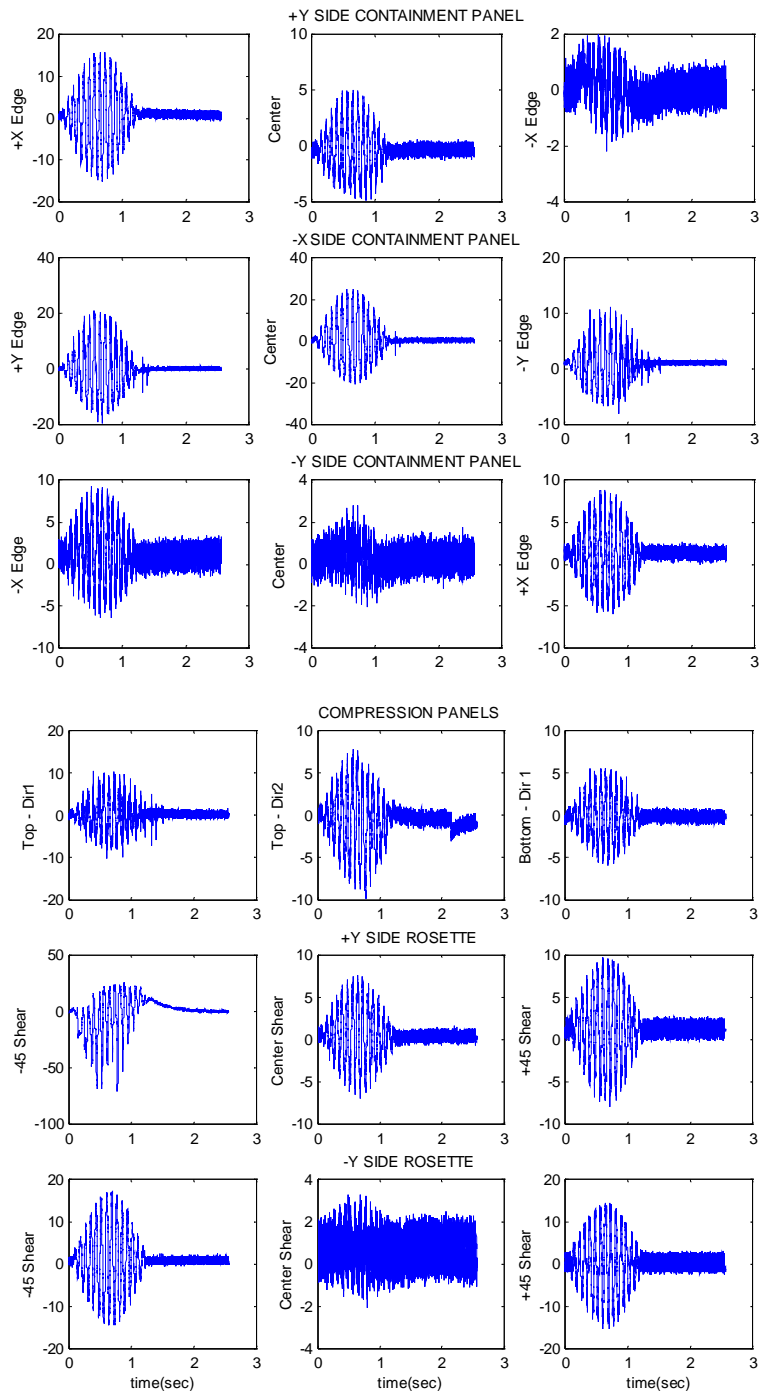


Response along the +X side edge of the top compression panel

17. Appendix E: Strain Results from the Full Amplitude Sine Burst Test

In this section, a collection of plots is shown that illustrate the calorimeter strain response as measured by the strain gage sensors. The time history plots are shown for the sine burst tests along both axes. The strains are measured in units of micro-strains.

17.1 Transverse Axis Results



17.2 Thrust Axis Results

